81-8-209

DEUTSCHES ELEKTRONEN-SYNCHROTRON DESY

DESY 81-043
July 1981

HELICITY DESCRIPTION OF $e^+e^- \to q\bar{q}g$ AND $e^+e^- \to Q\bar{Q}(1^{--}) \to ggg$ ON AND OFF THE Z^0: QUARK, GLUON AND BEAM POLARIZATION EFFECTS

by

Jürgen G. Körner
Deutsches Elektronen-Synchrotron DESY, Hamburg

D. H. Schiller
Fachbereich Physik, Universität Siegen

NOTKESTRASSE 85 · 2 HAMBURG 52

To be sure that your preprints are promptly included in the
HIGH ENERGY PHYSICS INDEX ,
send them to the following address (if possible by air mail) :

DESY
Bibliothek
Notkestrasse 85
2 Hamburg 52
Germany

DESY 81-043
July 1981

Helicity Description of $e^+e^- \to q\bar{q}g$ and $e^+e^- \to Q\bar{Q}(1^{--}) \to ggg$ on and off the Z^0: Quark, Gluon and Beam Polarization Effects

Jürgen G. Körner

Deutsches Elektronen-Synchrotron DESY, Hamburg

D.H. Schiller

Fachbereich Physik, Universität Siegen

Abstract

We develop the helicity description for the processes $e^+e^- \to q\bar{q}g$ and $e^+e^- \to Q\bar{Q}(1^{--}) \to ggg$ (γgg) in the purely electromagnetic case, in the γ-Z^0 interference region and on the Z^0-pole. We present complete differential cross section formulas including beam, quark and gluon polarization effects. We also treat the corresponding processes $e^+e^- \to q\bar{q}S$ and $e^+e^- \to Q\bar{Q}(1^{--}) \to SSS(\gamma SS)$ involving scalar gluons.

1. Introduction

The observation of p_T-broadening effects in jets produced in e^+e^--interactions [1] have been successfully interpreted in terms of hard gluon emission from primordially produced quarks. Similarly, the observed decay pattern of the $\Upsilon(9.47)$ shows consistency with the three gluon decay picture predicted by QCD [2]. These two experiments have been keystones in our growing belief that QCD is the underlying theory of strong interactions.

The two fundamental QCD processes $e^+e^- \to q\bar{q}g$ and $e^+e^- \to Q\bar{Q}(1^{--}) \to ggg(\gamma gg)$ will continue to be at the focus of experimental investigations in the coming years. As more data becomes available one will be able to test more details of the underlying QCD processes, as e.g. the predicted angular beam-event correlations [3,4].These tests can be further refined by the use of transversely and/or longitudinally polarized beams expected to be available in the near future. Also, when the energy range of e^+e^--machines is extended upwards, data will become available in the γ-Z^0 interference region and eventually on the Z^0-pole. This opens the possibility for further QCD-tests involving parity-violating interactions. Finally, the QCD processes result in definite predictions for the polarization of the produced quarks and gluons (photons) which may eventually become testable.

Basically it is quite straightforward to derive the necessary cross-section and polarization formulas from the underlying QCD Born term Feynman diagrams. Traditionally, the necessary formulas have been derived by using the "trace" method. The Feynman diagram contributions are squared and traces are taken over the product of γ-matrices appearing in the squared expressions with appropriate covariant polarization vectors included if desired. These trace calculations can become quite tedious when parity violating and/or

polarization effects are included. Also, in doing the lengthy trace calculations, one is always in danger of loosing contact with the basic physics of the process.

In this paper we advocate the use of the helicity formalism for the initial and final state quanta and illustrate its numerous advantages. * Once the relevant Born term helicity amplitudes have been calculated one can obtain from these within a few lines all cross-section and polarization formulas. Parity-violating effects are easily handled since the replacement $\gamma_\mu \to \gamma_\mu\gamma_5$ results in mere sign changes in some of the helicity amplitudes when the quarks are massless, as is assumed throughout this paper. Since the helicity amplitudes have a direct physical interpretation the physics remains transparent at every step of the calculation. In particular, soft-collinear gluon singularities can be easily isolated since they occur only in a few helicity amplitudes. Finally, our helicity amplitudes are necessary input to event generation programs which attempt to incorporate helicity dependent fragmentation processes.

In the course of developing our helicity formalism for quark and gluon polarization we comprehensively rederive cross-section formulas which have already appeared in scattered places in the literature. Most of our polarization pre-

* For higher order multijet processes with many contributing Feynman tree diagrams it may even become mandatory to use the helicity method. Cross-section expressions which are a sum of squares of helicity amplitudes are much easier to handle than the corresponding cross-section expressions using the trace method which are traces of the square of a sum of Feynman diagrams. The symbolic computer manipulations necessary in the latter calculation can quickly become unmanageable even for big computers. Furthermore, since the on-mass-shell gluons propagate only with their transverse spin degrees of freedom in the helicity treatment, one avoids the necessity of including ghost contributions.

dictions are new.

We organize our paper as follows. In Sec. 2 we discuss the general structure of the differential e^+e^- cross-section in the presence of beam polarization including p.v. effects. Our treatment very closely follows the general approach developed in [5] which is, however, adapted to our specific needs. In order to be selfcontained and readable it was necessary to duplicate some of the material contained in [5] The differential cross-section (density matrix) is expanded into the maximal set of independent hadronic correlation cross-sections (hadronic correlation density matrices) with the coefficients depending on i) angular factors describing the relative orientation of the initial beam system and the final hadron event system ii) beam polarization parameters and iii) the electro-weak coupling parameters of the underlying theory of electro-weak interactions. The hadronic cross sections (density matrices) are then expressed as sums of bilinears of helicity amplitudes. We introduce and discuss the structure of final state polarization parameters. Sec. 3 is devoted to the process $e^+e^- \to q\bar{q}g$. We compute the Born term helicity amplitudes for some specific event coordinate systems and use these to calculate cross section and quark and gluon polarization formulas. Sec. 4 is devoted to the process $e^+e^- \to Q\bar{Q}(1^{--}) \to ggg(\gamma gg)$. Sec. 5 contains some concluding remarks.

We collect some material on helicity spinors and polarization vectors in Appendix A, and on the density matrix description of the gluon (photon) in Appendix B. In Appendix C we discuss general covariants and invariants for the process $e^+e^- \to q\bar{q}g$ and give the general helicity projection formula. In Appendix D we write down a set of transversity frame helicity amplitudes for $e^+e^- \to q\bar{q}g$. In Appendix E we finally present results on the helicity formalism for the processes $e^+e^- \to q\bar{q}S$ and $e^+e^- \to Q\bar{Q}(1^{--}) \to SSS$ (γSS) involving scalar gluons.

2. Cross sections and density matrices.

The general cross section for $e^+e^- \to \gamma, Z^0 \to$ hadrons can be written as a linear superposition of the various parity conserving (p.c.) and parity violating (p.v.) terms in the hadron tensors $H^{JJ'}_{\mu\nu}$ and lepton tensors $L^{JJ'}_{\mu\nu}$. One defines four hermitian hadron tensors $H^r_{\mu\nu}$ (r = 1, ..., 4) by [5]

$$
\begin{aligned}
H^1_{\mu\nu} &= \tfrac{1}{2}\left(H^{VV}_{\mu\nu} + H^{AA}_{\mu\nu}\right) = H^{RR}_{\mu\nu} + H^{LL}_{\mu\nu}\,, \\
H^2_{\mu\nu} &= \tfrac{1}{2}\left(H^{VV}_{\mu\nu} - H^{AA}_{\mu\nu}\right) = H^{LR}_{\mu\nu} + H^{RL}_{\mu\nu}\,, \\
H^3_{\mu\nu} &= \tfrac{i}{2}\left(H^{VA}_{\mu\nu} - H^{AV}_{\mu\nu}\right) = i\left(H^{LR}_{\mu\nu} - H^{RL}_{\mu\nu}\right), \\
H^4_{\mu\nu} &= \tfrac{1}{2}\left(H^{VA}_{\mu\nu} + H^{AV}_{\mu\nu}\right) = H^{RR}_{\mu\nu} - H^{LL}_{\mu\nu}\,,
\end{aligned}
\qquad (2.1)
$$

and accordingly four lepton tensors $L^r_{\mu\nu}$. The superscripts V and A denote the contributions of the vector ($V_\mu = \langle f|J^V_\mu(0)|0\rangle$) and axial-vector ($A_\mu = \langle f|J^A_\mu(0)|0\rangle$) currents according to $H^{JJ'}_{\mu\nu} = \langle J_\mu J'^*_\nu \rangle$, (J,J' = V,A), where <...> means sum over the (final state) polarizations. The superscripts L and R, on the other hand, refer to the contributions of left-handed ($2L_\mu = V_\mu - A_\mu$) and right-handed ($2R_\mu = V_\mu + A_\mu$) currents used especially in neutrino interactions. In e^+e^- annihilation, however, the representation in terms of V- and A-contributions is more convenient. Similar definitions apply to the lepton tensors $L^r_{\mu\nu}$ with currents given explicitly by $j^V_\mu = \bar{v}(p_+)\gamma_\mu u(p_-)$ and $j^A_\mu = \bar{v}(p_+)\gamma_\mu\gamma_5 u(p_-)$.

The cross section can then be written in a matrix factorized form as

$$
d\sigma = \left(\frac{2\pi\alpha}{s}\right)^2 \sum_{r',r=1}^{4} g_{r'r}(s)\, L^{r'} \cdot H^r \; dLIPS\,, \qquad (2.2)
$$

where $\alpha = 1/137$ is the fine structure constant, $s = 4E^2_{beam}$ the total c.m. energy squared, dLIPS the Lorentz-invariant phase space element and L.H stands for

$L_{\mu\nu}\, H^{\mu\nu}$. The coefficients of the energy dependent electro-weak coupling matrix $g_{r'r}(s)$ are given in the next subsection. The factorized form (2.2) has the advantage that the various parts determining the cross section are separated into three pieces: $L^r_{\mu\nu}$ contains the angular dependences and the beam polarization parameters, $H^r_{\mu\nu}$ contains the hadron dynamics of the final state and $g_{r'r}(s)$ comprises the model dependent parameters of the underlying electro-weak theory.

We anticipate already here that the two cases discussed in the main part of this paper do not require the full hadronic structure of (2.1). In the case $e^+e^- \to q\bar{q}g$ with massless quarks one has from γ_5-invariance $H^{VV}_{\mu\nu} = H^{AA}_{\mu\nu}$ and $H^{VA}_{\mu\nu} = H^{AV}_{\mu\nu}$ so that the only nonvanishing elements are $H^1_{\mu\nu}$ and $H^4_{\mu\nu}$, whereas in the case $e^+e^- \to Q\bar{Q}(1^{--}) \to ggg$ only $H^{VV}_{\mu\nu}$ contributes so that the nonvanishing elements are $H^1_{\mu\nu} = H^2_{\mu\nu}$.

Electro-Weak Coupling Matrix

The electro-weak coupling matrix $g_{r'r}(s)$ entering (2.2) is given by [5]

$$
\begin{aligned}
g_{\substack{11\\12}} &= Q_f^2 - 2Q_f v v_f \,\mathrm{Re}\,\chi_Z + (v^2+a^2)(v_f^2 \pm a_f^2)\,|\chi_Z|^2 ,\\
g_{\substack{13\\23}} &= -2Q_f v a_f \,\mathrm{Im}\,\chi_Z ,\\
g_{\substack{14\\24}} &= 2Q_f v a_f \,\mathrm{Re}\,\chi_Z - (v^2 \pm a^2)\, 2v_f a_f\,|\chi_Z|^2 ,\\
g_{\substack{21\\22}} &= Q_f^2 - 2Q_f v v_f \,\mathrm{Re}\,\chi_Z + (v^2-a^2)(v_f^2 \pm a_f^2)\,|\chi_Z|^2 ,\\
g_{\substack{31\\32}} &= -2Q_f a v_f \,\mathrm{Im}\,\chi_Z ,\\
g_{33} &= 2Q_f a a_f \,\mathrm{Re}\,\chi_Z ,\\
g_{\substack{34\\43}} &= 2Q_f a a_f \,\mathrm{Im}\,\chi_Z ,\\
g_{\substack{41\\42}} &= 2Q_f a v_f \,\mathrm{Re}\,\chi_Z - 2va\,(v_f^2 \pm a_f^2)\,|\chi_Z|^2 ,\\
g_{44} &= -2Q_f a a_f \,\mathrm{Re}\,\chi_Z + 4va\, v_f a_f\,|\chi_Z|^2 ,
\end{aligned}
\qquad (2.3)
$$

where $\chi_Z(s) = gM_Z^2 s(s-M_Z^2 + iM_Z\Gamma_Z)^{-1}$, with M_Z and Γ_Z the mass and width of the Z^o and $g = G_F(8\sqrt{2}\pi\alpha)^{-1} \approx 4.49 \cdot 10^{-5}\,\mathrm{GeV}^{-2}$. Q_f are the charges of the final state quarks to which the electro-weak currents directly couple; v and a, and v_f and a_f are the electro-weak vector and axial vector coupling constants. For example, in the Weinberg-Salam model, one has $v = -1 + 4\sin^2\theta_W$, $a = -1$ for leptons, $v_f = 1 - \frac{8}{3}\sin^2\theta_W$ and $a_f = 1$ for u, c, t...quarks ($Q_f = 2/3$) and $v_f = -1 + \frac{4}{3}\sin^2\theta_W$ and $a_f = -1$ for d, s, b... quarks ($Q_f = -1/3$). The left- and right-handed coupling constants are then given by $g_L = v + a$ and $g_R = v - a$, respectively. In the purely electromagnetic case one has $g_{11} = g_{12} = g_{21} = g_{22} = Q_f^2$ and all other $g_{r'r} = 0$. The terms going with $\mathrm{Re}\,\chi_Z$ and $\mathrm{Im}\,\chi_Z$ come from γ-Z interference, whereas the terms with $|\chi_Z|^2$ are the purely weak ones.

Lepton Tensor

The lepton tensors $L^r_{\mu\nu}$ take their simplest form in a beam specific c.m. coordinate system Ox'y'z' denoted by a prime in the following. We choose the z'-axis to be along the e^--direction and, for definiteness, the x'-axis is taken to lie in the plane of the accelerator pointing inward (along the Lorentz force). Since the lepton tensors $L^{JJ'}_{\mu\nu}$ are essentially the density matrices of the virtual γ and Z^o in $e^+e^- \to \gamma^*$ and $e^+e^- \to Z^o$, they can be calculated according to the general formula

$$
L^{JJ'}_{\mu\nu} = \frac{1}{2S}\sum_{\lambda_+\lambda'_+} j^J_{\mu;\lambda_+\lambda_-}\, \rho^+_{\lambda_+\lambda'_+}\, \rho^-_{\lambda_-\lambda'_-}\, j^{J'*}_{\nu;\lambda'_+\lambda'_-} \qquad (J,J' = V,A) \qquad (2.4)
$$

where $\rho^\pm$ is the helicity density matrix of the initial $e^\pm$ and $j^J_{\mu;\lambda_+\lambda_-} = \langle o|j^J_\mu(o)|e^+(\lambda_+)e^-(\lambda_-)\rangle$ are the helicity amplitudes. Using the helicity bispinors defined in Appendix A we find in the beam frame Ox'y'z'.

$$
j^V_{\mu;\lambda_+\lambda_-} = \bar{v}(p_+\lambda_+)\gamma_\mu u(p_-\lambda_-) = \begin{cases} -\sqrt{s}\,(\sigma_\mu)_{\lambda_+\lambda_-} & \mu = 1,2 \\ 0 & \mu = 0,3 \end{cases}
$$

$$
j^A_{\mu;\lambda_+\lambda_-} = \bar{v}(p_+\lambda_+)\gamma_\mu\gamma_5 u(p_-\lambda_-) = \begin{cases} -\sqrt{s}\,(\sigma_\mu\sigma_3)_{\lambda_+\lambda_-} & \mu = 1,2 \\ 0 & \mu = 0,3 \end{cases} \qquad (2.5)
$$

where σ_μ (μ = 1,2,3) are the usual Pauli matrices. The fact that these amplitudes vanish for μ = 0,3 is due to current conservation and to the chirality preserving interactions γ_μ and $\gamma_\mu\gamma_5$ for massless leptons. As a consequence, only the components $L^r_{\mu\nu}$ with μ,ν = 1, 2 are nonvanishing (in the beam frame Ox'y'z').

The helicity density matrices $\rho^\pm$ take the simple form

$$\rho^\pm = \frac{1}{2}\left(\mathbb{1} + \xi^\pm_{x_\pm}\sigma_1 + \xi^\pm_{y_\pm}\sigma_2 + \xi^\pm_{z_\pm}\sigma_3\right),$$

if the components of the rest frame polarization vector $\vec{\xi}^\pm$ of $e^\pm$ are referred to the helicity rest frame $Ox_\pm y_\pm z_\pm$ of $e^\pm$[6]. Since the $e^-(e^+)$ is moving along the positive (negative) z'-axis having polar and azimuthal angles $\theta_- = \varphi_- = 0$ ($\theta_+ = \varphi_+ = \pi$), the frame $Ox_-y_-z_-$ ($Ox_+y_+z_+$) is obtained - apart from a boost along the z'-axis - from the beam frame Ox'y'z' by rotating the latter through $R_-(o,o,o)$ ($R_+(\pi,\pi,-\pi)$) in accordance with the rotation $R(\varphi,\theta,-\varphi)$ used to define the helicity states in Appendix A. From the orientation of the frames shown in Fig.1 it is then clear that $\rho^\pm$ can be written as

$$\rho^-_{\lambda_-\lambda'_-} = \frac{1}{2}\left(\mathbb{1} + \xi^-_{x'}\sigma_1 + \xi^-_{y'}\sigma_2 + \xi^-_{z'}\sigma_3\right)_{\lambda_-\lambda'_-},$$

$$\rho^+_{\lambda_+\lambda'_+} = \frac{1}{2}\left(\mathbb{1} - \xi^+_{x'}\sigma_1 + \xi^+_{y'}\sigma_2 - \xi^+_{z'}\sigma_3\right)_{\lambda_+\lambda'_+}, \qquad (2.6)$$

where the components $\xi^\pm_n$, (n = x,y,z) now refer to the laboratory beam frame Ox'y'z'. Thus $\xi^\pm_x$, and $\xi^\pm_y$, denote the transverse beam polarization in and out of the accelerator plane, and $\xi^\pm_z$, ($=\mp h^\pm$) the longitudinal polarization (helicity) of $e^\pm$. For natural transverse beam polarization of degree P one has $\vec{\xi}^\pm = (0,\pm P,0)$. Using (2.5) and (2.6) in (2.4), we find for the nonvanishing elements of the lepton tensors $L^r_{\mu\nu}$ (defined analogously as in (2.1))

$$L'^1_{11} = L'^1_{22} = (1 - h^-h^+), \qquad (s)$$
$$L'^1_{12} = -L'^1_{21} = -i(h^- - h^+); \qquad (a)$$

$$L'^2_{11} = -L'^2_{22} = -\left(\xi^-_{x'}\xi^+_{x'} - \xi^-_{y'}\xi^+_{y'}\right), \qquad (s)$$
$$L'^2_{12} = L'^2_{21} = -\left(\xi^-_{x'}\xi^+_{y'} + \xi^-_{y'}\xi^+_{x'}\right); \qquad (s)$$

$$L'^3_{11} = -L'^3_{22} = \left(\xi^-_{x'}\xi^+_{y'} + \xi^-_{y'}\xi^+_{x'}\right), \qquad (s)$$
$$L'^3_{12} = L'^3_{21} = -\left(\xi^-_{x'}\xi^+_{x'} - \xi^-_{y'}\xi^+_{y'}\right); \qquad (s)$$

$$L'^4_{11} = L'^4_{22} = (h^- - h^+), \qquad (s)$$
$$L'^4_{12} = -L'^4_{21} = -i(1 - h^-h^+). \qquad (a)$$

(2.7)

Here we have indicated the $\mu \leftrightarrow \nu$ symmetry properties (s = symmetric, a = antisymmetric) of the various components of $L'_{\mu\nu}$ which will be of later convenience when considering the contraction with the hadronic tensor.

Hadron Tensor

In the overall c.m. system that we are considering only the space components of the four hadron tensors H^r_{mn} (m,n = 1,2,3) contribute to the annihilation cross section (2.2). Also, since the spin averaged hadron tensors H^r_{mn} are hermitian, there are in general nine real independent components H^r_{mn} for each r = 1,2,3,4. We introduce the following real six symmetric and three antisymmetric combinations under $m \leftrightarrow n$ (dropping the superscript r for compactness)

$$
\begin{aligned}
\sigma_U &= H_{++} + H_{--} && = H_{11} + H_{22} && (s)\\
\sigma_L &= H_{00} && = H_{33} && (s)\\
\sigma_T &= \tfrac{1}{2}\left(H_{+-} + H_{-+}\right) && = \tfrac{1}{2}\left(-H_{11} + H_{22}\right) && (s)\\
\sigma_4 &= \tfrac{-i}{2}\left(H_{+-} - H_{-+}\right) && = -\tfrac{1}{2}\left(H_{12} + H_{21}\right) && (s)\\
\sigma_5 &= \tfrac{-i}{4}\left(H_{+0} - H_{0+} + H_{-0} - H_{0-}\right) && = \tfrac{-1}{2\sqrt{2}}\left(H_{23} + H_{32}\right) && (s)\\
\sigma_I &= \tfrac{1}{4}\left(H_{+0} + H_{0+} - H_{-0} - H_{0-}\right) && = \tfrac{-1}{2\sqrt{2}}\left(H_{31} + H_{13}\right) && (s)\\
\sigma_7 &= H_{++} - H_{--} && = -i\left(H_{12} - H_{21}\right) && (a)\\
\sigma_8 &= \tfrac{1}{4}\left(H_{+0} + H_{0+} + H_{-0} + H_{-0}\right) && = \tfrac{-i}{2\sqrt{2}}\left(H_{23} - H_{32}\right) && (a)\\
\sigma_9 &= \tfrac{-i}{4}\left(H_{+0} - H_{0+} - H_{-0} + H_{0-}\right) && = \tfrac{-i}{2\sqrt{2}}\left(H_{31} - H_{13}\right) && (a)
\end{aligned}
\qquad (2.8)
$$

where $H_{\sigma\sigma'} \equiv \epsilon^{\mu}_{\sigma} H_{\mu\nu} \epsilon^{*\nu}_{\sigma'}$, $(\sigma,\sigma' = 0,\pm)$, with ϵ^{μ}_{σ} given in (A.8).

In order to deal with the final state polarization phenomena considered in this paper we have written (2.8) in a form appropriate for generalization to density matrices, i.e. we have not used the relations $H_{+-} + H_{-+} = 2\mathrm{Re}H_{+-}$, etc. valid in the spin-averaged case, since they are no longer true for general density matrix elements. The generalization fo final state density matrices is straightforward and consists, for the three-particle final states considered here, in the replacement

$$
H_{\sigma\sigma'} = \sum_{\lambda_1\lambda_2\lambda_3} \left(\mathbb{H}_{\sigma\sigma'}\right)_{\lambda_1\lambda_2\lambda_3;\lambda_1\lambda_2\lambda_3} \longrightarrow \left(\mathbb{H}_{\sigma\sigma'}\right)_{\lambda_1\lambda_2\lambda_3;\lambda'_1\lambda'_2\lambda'_3} , \qquad (2.9)
$$

where the λ_i denote the helicities of the final state quanta. In terms of the vector and axial-vector helicity amplitudes given by

$$
F^{J}_{\lambda_1\lambda_2\lambda_3;\sigma} \equiv \langle \lambda_1\lambda_2\lambda_3 \,|\, J^{J}_{\mu}(0) \,|0\rangle\, \epsilon^{\mu}_{\sigma} = J_{\mu}\epsilon^{\mu}_{\sigma} \qquad (J = V, A) \qquad (2.10)
$$

the hadronic tensor density matrix reads

$$
\left(\mathbb{H}^{JJ'}_{\sigma\sigma'}\right)_{\lambda_1\lambda_2\lambda_3;\,\lambda'_1\lambda'_2\lambda'_3} = F^{J}_{\lambda_1\lambda_2\lambda_3;\sigma}\; F^{J'\,*}_{\lambda'_1\lambda'_2\lambda'_3;\,\sigma'} \qquad (J,J' = V, A) \qquad (2.11)
$$

Contracting with the lepton tensors according to (2.2) gives the most general final state density matrix (unnormalized). In this paper, however, we limit our attention to single particle density matrices where the helicities of the remaining particles have been summed over. For spin-1/2 or massless spin-1 particles these can be conveniently parametrized in terms of the unit and Pauli matrices as

$$
\left(\mathbb{H}_{\alpha}\right)_{\lambda\lambda'} = \frac{1}{2}\left(\sigma_{\alpha}\,\mathbb{1} + \rho_{\alpha x}\,\sigma_1 + \rho_{\alpha y}\,\sigma_2 + \rho_{\alpha z}\,\sigma_3\right), \qquad (2.12)
$$

where α = U, L, ... 9 denotes one of the nine combinations of $\mathbb{H}_{\sigma\sigma'}$, defined as in (2.8) and $\sigma_{\alpha} = \mathrm{Tr}\,\mathbb{H}_{\alpha}$ are the spin-averaged (hadronic) correlation cross sections (2.8). The three-component object $\vec{\rho}_{\alpha}$ is the (hadronic) correlation polarization vector in the quark case and the correlation Stokes vector in the gluon case. After contraction with the lepton tensors the $\vec{\rho}_{\alpha}$'s build up the unnormalized polarization (or Stokes) vector in much the same way as the σ_{α}'s build up the unpolarized cross section [5].

Angular Correlations

We are now in the position to consider the beam-event correlations that arise from the contraction of the lepton and hadron tensors. First, we have to rotate the lepton tensors L'_{mn} given in (2.7) to the event frame. This is achieved by the Euler rotation illustrated in Fig.2

$$L_{k\ell}(\varphi,\theta,\chi) = R_{km}(\varphi,\theta,\chi)\, R_{\ell n}(\varphi,\theta,\chi)\, L'_{mn} \qquad (2.13)$$

where φ, θ, χ are the Euler angles describing the rotation from the beam-system to the event-system. Details of the calculation are given in [5]. Let us note, though, that the contraction $L_{mn}(\varphi,\theta,\chi)\, H_{mn}$ is simplified by separately considering the symmetric and antisymmetric parts of L_{mn} and H_{mn} according to the classification after (2.7) and (2.8). Such symmetry considerations are also very helpful when one wants to assess quickly the influence of beam polarization on the measurement of the various hadron tensor components. One obtains (omitting again the superscript r and the helicity indices on $(H^{r}_{\alpha})_{\lambda\lambda'}$):

$$\begin{aligned}
\tfrac{3}{4} L^{1}_{mn} H_{mn} &= (1-h^{-}h^{+})\, H_A + (h^{-}-h^{+})\, H_D \\
\tfrac{3}{4} L^{2}_{mn} H_{mn} &= X(\varphi)\, H_B + Y(\varphi)\, H_C \\
\tfrac{3}{4} L^{3}_{mn} H_{mn} &= X(\varphi)\, H_C - Y(\varphi)\, H_B \\
\tfrac{3}{4} L^{4}_{mn} H_{mn} &= (1-h^{-}h^{+})\, H_D + (h^{-}-h^{+})\, H_A
\end{aligned} \qquad (2.14)$$

where

$$\begin{aligned}
H_A &= \tfrac{3}{8}(1+\cos^2\theta)\, H_U + \tfrac{3}{4}\sin^2\theta\, H_L + \tfrac{3}{4}\sin^2\theta\cos 2\chi\, H_T \\
&\quad - \tfrac{3}{4}\sin^2\theta\sin 2\chi\, H_4 + \tfrac{3}{2\sqrt{2}}\sin 2\theta\sin\chi\, H_5 - \tfrac{3}{2\sqrt{2}}\sin 2\theta\cos\chi\, H_I \,, \\
H_B &= \tfrac{3}{8}\sin^2\theta\, H_U - \tfrac{3}{4}\sin^2\theta\, H_L + \tfrac{3}{4}(1+\cos^2\theta)\cos 2\chi\, H_T \\
&\quad - \tfrac{3}{4}(1+\cos^2\theta)\sin 2\chi\, H_4 - \tfrac{3}{2\sqrt{2}}\sin 2\theta\sin\chi\, H_5 + \tfrac{3}{2\sqrt{2}}\sin 2\theta\cos\chi\, H_I \,, \\
H_C &= \tfrac{3}{2}\cos\theta\sin 2\chi\, H_T + \tfrac{3}{2}\cos\theta\cos 2\chi\, H_4 \\
&\quad + \tfrac{3}{\sqrt{2}}\sin\theta\cos\chi\, H_5 + \tfrac{3}{\sqrt{2}}\sin\theta\sin\chi\, H_I \,, \\
H_D &= \tfrac{3}{4}\cos\theta\, H_7 - \tfrac{3}{\sqrt{2}}\sin\theta\cos\chi\, H_8 + \tfrac{3}{\sqrt{2}}\sin\theta\sin\chi\, H_9 \,,
\end{aligned} \qquad (2.15)$$

with all hadron tensors referring to the event system and

$$\begin{aligned}
X(\varphi) &= (\xi^{-}_{x'}\xi^{+}_{x'} - \xi^{-}_{y'}\xi^{+}_{y'})\cos 2\varphi + (\xi^{-}_{x'}\xi^{+}_{y'} + \xi^{-}_{y'}\xi^{+}_{x'})\sin 2\varphi \,, \\
Y(\varphi) &= -(\xi^{-}_{x'}\xi^{+}_{x'} - \xi^{-}_{y'}\xi^{+}_{y'})\sin 2\varphi + (\xi^{-}_{x'}\xi^{+}_{y'} + \xi^{-}_{y'}\xi^{+}_{x'})\cos 2\varphi \,.
\end{aligned} \qquad (2.16)$$

Note that H_B and H_C contain no more hadronic structure than H_A. This means that the presence of transverse beam polarization does not increase the number of possible hadronic measurements. On the other hand, transverse beam polarization is helpful in disentangling the hadronic structure.

Equation (2.14) gives the most general structure of possible beam-event correlations in the presence of beam polarization and final state polarisation effects. The whole angular dependence on the relative beam-event angles φ, θ and χ is explicitly exhibited in (2.15), since the hadronic density matrices H_α are evaluated in the event frame and thus are independent of φ, θ and χ. In the case of the one-particle density matrix (2.12), this means that σ_α and $\vec{\rho}_\alpha$ appear with the same angular coefficients. Thus, the angular dependence of the unnormalized polarization (Stokes) vector is obtained from that of the unpolarized cross section by the formal substitution $\sigma_\alpha \to \vec{\rho}_\alpha$! It is clear that for specific applications the complexity of (2.14) is considerably reduced.

Event Coordinate Systems

Two types of event coordinate systems have proved useful in the analysis of three-jet events in e^+e^--interactions. In the helicity system the event z-axis is chosen to lie in the event plane, and in the transversity frame the z-axis is chosen normal to the event plane. The Euler angles φ, θ, χ connecting the beam coordinate system (x'y'z') with the event coordinate system (x,y,z) are illustrated in Fig.2 and have the following meaning:

(i) Helicity system. φ is the azimuthal angle between the storage ring plane (x', z') and the (z', z) plane; χ is the azimuthal angle between the (z',z) plane and the (x,z) event plane; θ is the polar angle between the z' beam axis and the z event axis.

(ii) Transversity system. The Euler angles are denoted as $\bar{\varphi}$, $\bar{\theta}$, $\bar{\chi}$: $\bar{\varphi}$ is the azimuthal angle between the storage ring plane (x',z') and the (z', z) plane; $\bar{\chi}$ is the azimuthal angle between the (z', z) plane and the plane (x,z) perpendicular to the event plane; $\bar{\theta}$ is the polar angle between the z' beam axis and the normal to the event plane z. The relations (2.14) - (2.16) hold true with φ, θ, χ replaced by $\bar{\varphi}$, $\bar{\theta}$, $\bar{\chi}$.

The two systems are in turn connected by an Euler rotation $R(-\frac{\pi}{2}, -\frac{\pi}{2}, 0)$ which allows one to relate the hadron tensor components in the two event frames. One has [5]

$$
\begin{aligned}
\bar{H}_U &= \tfrac{1}{2} H_U + H_L - H_T \,, \\
\bar{H}_L &= \tfrac{1}{2} H_U + H_T \,, \\
\bar{H}_T &= \tfrac{1}{4} H_U - \tfrac{1}{2} H_L - \tfrac{1}{2} H_T \,, \\
\bar{H}_4 &= \sqrt{2}\, H_I \,, \\
\bar{H}_5 &= \tfrac{1}{\sqrt{2}} H_4 \,, \\
\bar{H}_I &= H_5 \,, \\
\bar{H}_7 &= 2\sqrt{2}\, H_9 \,, \\
\bar{H}_8 &= \tfrac{1}{2\sqrt{2}} H_7 \,, \\
\bar{H}_9 &= H_8 \,,
\end{aligned}
\qquad (2.17)
$$

where the $\bar{H}_\alpha$ refer to the hadron tensor components in the transversity frame*.

* More precisely, we have rotated only the indices σ,σ' of the virtual photon (or Z^0) so that the λ -indices on both, $(H_\alpha)_{\lambda\lambda'}$ and $(\bar{H}_\alpha)_{\lambda\lambda'}$, are the same (unchanged) helicities of the final state quanta. On the level of helicity amplitudes (2.10) we have $\bar{F}_{\lambda_1\lambda_2\lambda_3;\tau} = F_{\lambda_1\lambda_2\lambda_3;\sigma} D^1_{\sigma\tau}(-\pi/2, -\pi/2, 0)$, where $\sigma(\tau)$ is a helicity (transversity) quantum number.

Before closing this section we want to make some clarifying remarks on the structure of the unpolarized three parton production cross sections in order to bring out their key features. The unpolarized cross-sections will be the most relevant to experimental analysis in the coming years. For the (planar) 3-jet final states one finds from reflection invariance in the event plane [5] that the number of nonvanishing cross-sections is considerably smaller than indicated by the general decomposition (2.8). For example, in the helicity system and for planar three-body events, parity invariance predicts [5] that the only nonvanishing cross-sections are $\sigma^{VV,AA}_{U,L,T,I,9}$ and $\sigma^{VA,AV}_{4,5,7,8}$. Furthermore, in the Born approximation $\sigma^{VV,AA}_{9}$ and $\sigma^{VA,AV}_{4,5}$ vanish, which is easy to see from the helicity amplitudes in Table 1 since the Born term helicity amplitudes are real (see also Sec.3)*. Thus, to $O(\alpha_s)$ and in the mass zero case where $\sigma^{VV}_\alpha = \sigma^{AA}_\alpha$ and $\sigma^{VA}_\alpha = \sigma^{AV}_\alpha$ the unpolarized hadron tensor has only 6 independent components**. Similarly, the number of independent components in the Born approximation to $e^+e^- \to Q\bar{Q}(1^{--}) \to ggg$ is only 4. Although the above statements are specific to the helicity event coordinate system, a covariant analysis will of course lead to the same denumeration [8] as will an analysis in any other coordinate system, as e.g. the transversity system [5]. Similar parity relations hold for the single-particle polarization (Stokes) vector components which will be commented on in the next sections.

* In a more general language these cross sections are T-odd quantities which do not receive contributions from real Born term processes (see e.g. [7]).

** This result holds true also to $O(\alpha_s^2)$ as shown in Ref.[8], where the imaginary parts of the one-loop contributions were calculated in order to determine σ^{VV}_α to $O(\alpha_s^2)$. σ^{VV}_9 was found to be zero in the massless limit. The same statement holds true for σ^{AA}_9 and $\sigma^{VA,AV}_{4,5}$ due to γ_5-invariance. A heuristic explanation is given by the following chain of arguments. The imaginary part of the 1-loop

3. $e^+e^- \to q\bar{q}g$

a) Helicity amplitudes.

From the Feynman diagrams Fig.3 one calculates the vector current amplitude

$$V^\mu = g_s \frac{\lambda^i}{2} \epsilon_\nu^*(p_3)\, \bar{u}(p_1)\Big[-\gamma^\nu \frac{\not p_1+\not p_3}{(p_1+p_3)^2}\gamma^\mu + \gamma^\mu \frac{\not p_2+\not p_3}{(p_2+p_3)^2}\gamma^\nu\Big] v(p_2)\,, \tag{3.1}$$

where g_s is the usual QCD coupling constant and λ^i are the Gell-Mann matrices of colour SU(3). The corresponding axial vector current amplitude A^μ is given by the replacement $v \to \gamma_5 v$.

We calculate helicity amplitudes in c.m. coordinate systems with the (x,z)-plane in the event plane (helicity system) and the y-axis perpendicular to the event plane.* There are 6 different choices of event-coordinate systems that we will consider:

Ia,b:	q along z;	(a)$\bar{q}$	(b)g	in (pos.x;z)-half-plane,
IIa,b:	$\bar{q}$ along z;	(a)g	(b)q	in (pos.x;z)-half-plane,
IIIa,b:	g along z;	(a)q	(b)$\bar{q}$	in (pos.x;z)-half-plane.

(3.2)

These event coordinate systems have been introduced in [3] in order to be able to perform the thrust analysis of beam-event correlations in $e^+e^- \to q\bar{q}g$.

The frames b are obtained from the frames a by a rotation $R_z(\pi)$, whereas the different frames a (or b) are related among one another by rotations $R_y(\theta_{ij})$, where θ_{ij} is the angle between particles i and j. In terms of the scaled energies x_i ($x_1 + x_2 + x_3 = 2$) one has

$$\sin\frac{\theta_{ij}}{2} = \big[(1-x_k)/x_i x_j\big]^{1/2} \qquad (k \neq i,j)\,,$$
$$\cos\frac{\theta_{ij}}{2} = \big[(1-x_i)(1-x_j)/x_i x_j\big]^{1/2}\,. \tag{3.3}$$

These relations are useful in evaluating the helicity amplitudes. Using the helicity spinors and vectors given in Appendix A one can calculate the Born term helicity amplitudes using the Feynman amplitude (3.1). The Born term helicity amplitudes in each of the six coordinate systems (3.2) are listed in Table I. Note that there are only six independent helicity amplitudes in the massless case since helicity cannot be flipped going from the quark to the antiquark (i.e. $\lambda_q = -\lambda_{\bar{q}}$) due to γ_5-invariance of the interaction. In Appendix C we have also worked out the helicity projection of a general set of invariant amplitudes for system IIa. We emphasize that the helicity amplitudes in helicity coordinate systems have the reality property of the underlying Feynman amplitude.

For massless quarks the axial vector helicity amplitudes $F^A_{\lambda_q\lambda_{\bar{q}}\lambda_g;\sigma}$ are related to the vector helicity amplitudes by the relations

$$F^A_{\lambda_q\lambda_{\bar{q}}\lambda_g;\,\sigma} = -2\lambda_{\bar{q}}\, F^V_{\lambda_q\lambda_{\bar{q}}\lambda_g;\,\sigma} \tag{3.4}$$

This is easy to see from (3.1) since massless Dirac spinors are eigenvectors of the γ_5-matrix, i.e. $\gamma_5 v_\pm = \mp v_\pm$.

The remaining 6 dependent helicity amplitudes can be obtained from the parity relations

$$F^V_{-\lambda_q-\lambda_{\bar{q}}-\lambda_g;\,0\,0}^{-1} = \pm F^V_{\lambda_q\lambda_{\bar{q}}\lambda_g;\,0\,0}^{+1} \tag{3.5}$$

Due to the simple charge conjugation property of the (massless!) Born amplitude (3.1) one can derive quark-antiquark exchange relations for

---

contributions is proportional to the singular part of the real 1-loop contributions. [8] The latter have the Born-term structure since the singularities arise from the integration region where the loop gluon is soft and collinear which, by heuristic reasoning, does not affect the spin structure of the underlying process. This implies that the imaginary part also has the Born term structure as has been explicitly verified in [8]. Consequently $\sigma_9^{VV,AA}$ and $\sigma_{4,5}^{VA,AV}$ are zero also to $O(\alpha_s^2)$. In Ref.[7] a similar calculation was done for $e^+e^- \to Q\bar{Q}(1^{--}) \to ggg$ with the result $\sigma_9^{VV} \neq 0$. In view of the conclusions of [8] the latter result should be reanalysed.

* Transversity frame helicity amplitudes are presented in Appendix D.

the Born term helicity amplitudes. These read:

$$F^{V,\,\mathrm{II}\,a\,(b)}_{\lambda_q\lambda_{\bar q}\lambda_g;\,\sigma}(x_1,x_2) = -F^{V,\,\mathrm{I}\,b\,(a)}_{\lambda_{\bar q}\lambda_q\lambda_g;\,\sigma}(x_2,x_1)\,,$$
$$F^{V,\,\mathrm{III}\,a}_{\lambda_q\lambda_{\bar q}\lambda_g;\,\sigma}(x_1,x_2) = -F^{V,\,\mathrm{III}\,b}_{\lambda_{\bar q}\lambda_q\lambda_g;\,\sigma}(x_2,x_1)\,. \qquad (3.6)$$

For the axial vector helicity amplitudes $F^{A}_{\lambda_q\lambda_{\bar q}\lambda_g;\sigma}$ one has the same relations as (3.5) and (3.6) but with opposite signs.

Looking at Table 1 one finds a very characteristic behaviour of the different helicity amplitudes in the soft-collinear gluon limit ($x_1 \to 1$ and $x_2 \to 1$) when the quark or antiquark momentum (systems I or II) is chosen as quantization axis. For definiteness we consider system I and approach the soft-collinear limit by taking the common (scaled) invariant mass (or off-mass-shellness) $\varepsilon = (1-x_1) = (1-x_2) = x_3/2$ to zero. As Table 1 shows, $F_{\frac12-\frac12\pm1;+i} \propto \varepsilon^{-1}$, $F_{\frac12-\frac12\pm1;0} \propto \varepsilon^{0}$ is constant and $F_{-\frac12\frac12\pm1;+1} \propto \varepsilon^{1}$ vanishes in this limit. This limiting behaviour is determined by the net helicity flip from the virtual photon to the $q\bar q$-system $|\lambda_q - \lambda_{\bar q} - \sigma|$. The singularity occurs only in the helicity amplitudes where no net helicity is flipped regardless of gluon helicities.* In the case where one or two units of net helicity are flipped, angular momentum factors cancel the propagator singularities and the corresponding helicity amplitudes are well behaved, respectively zero, in this limit. The singular helicity amplitudes are also the dominant ones over most of the phase space. Keeping only these would correspond to a variant of the leading-log approximation. They have the same quark-antiquark helicity structure as the lower order process $e^+e^- \to q\bar q$ which means that radiation of a soft-collinear gluon does not change the helicity structure of the quark (or antiquark) from which it is radiated. That the soft-collinear gluon limit of $e^+e^- \to q\bar q g$ reproduces the structure of $e^+e^- \to q\bar q$ has been remarked on before in [5,9]. A similar pattern is observed in system II. By contrast, in system III all helicity amplitudes have a singular ε^{-1}-behaviour.

*In the collinear limit $\theta_{13} \to 0$ or $\theta_{12} \to 0$ the singularity classification of the helicity amplitudes depends again only on the net helicity being flipped regardless of gluon helicities. In this case one does not, however, have the relation $F_{\frac12,-\frac12,1;1} = -F_{\frac12,-\frac12,-1;1}$ for the singular amplitudes in the soft gluon limit which implies the wellknown fact that a gluon radiated from a quark is 100% linearly polarized in the production plane in the soft gluon limit.

The singularity behaviour of the helicity amplitudes leads to a definite pattern of the soft-collinear behaviour of the correlation cross sections σ_α. These have been calculated according to their definition (2.8) for the six different helicity systems introduced in (3.2) and are listed in Table 2. The results agree with the corresponding expressions in [3]. Instead of listing σ_U separately in Table 2 we have given the total correlation cross section $\sigma = \sigma_U + \sigma_L$. It takes the well known form first presented in [10] and is frame independent since $\sigma = \sum_m \sum_\lambda (H^{VV}_{mm})_{\lambda\lambda}$ is rotationally invariant. The soft-collinear behaviour of σ_α can now be read off from Table 2. For example, for system I, one obtains $(\sigma^{VV}_U, \sigma^{VA}_7) \propto \varepsilon^{-2}$, $(\sigma^{VV}_I, \sigma^{VA}_8) \propto \varepsilon^{-1}$ and $(\sigma_L, \sigma_T) \propto \varepsilon^{0}$. Similar results hold for system II, whereas for system III all cross sections behave as ε^{-2}.

b) Quark density matrix.

As a next step we proceed to calculate the single particle spin density matrices. Let us first consider the quark correlation density matrix. Using the defining relations (2.12) one finds (for either system I, II or III):

$$(H^{VV}_\alpha)_{\lambda_q\lambda'_q} = \begin{cases} \frac12\left(\sigma^{VV}_\alpha \mathbb{1} + \vec{O}\cdot\vec{\sigma}\right) & \alpha = U,L,T,I \\ \frac12\left(O\,\mathbb{1} + \sigma^{VA}_\alpha \sigma_3\right) & \alpha = 7,8\,; \end{cases}$$
$$(H^{VA}_\alpha)_{\lambda_q\lambda'_q} = \begin{cases} \frac12\left(O\,\mathbb{1} + \sigma^{VV}_\alpha \sigma_3\right) & \alpha = U,L,T,I \\ \frac12\left(\sigma^{VA}_\alpha \mathbb{1} + \vec{O}\cdot\vec{\sigma}\right) & \alpha = 7,8\,, \end{cases} \qquad (3.7)$$

where σ^{VV}_α and σ^{VA}_α are the corresponding correlation cross sections given in Table 2. As mentioned above, quark and antiquark helicities are correlated in the mass zero limit ($\lambda_q = -\lambda_{\bar q}$), and thus the nondiagonal density matrix elements

are zero, i.e. $\rho_{\alpha x} = \rho_{\alpha y} = 0$. Consequently there is no quark transverse polarization component*. For the same reason one obtains the simple factorizing structure of (3.7). The fact that the p.c. (VV) part of the hadron tensor is unpolarized for the symmetric combinations U, L, T, I and longitudinally polarized for the antisymmetrie combinations 7, 8, and vice versa for the p.v. (VA) part is of course due to the parity classification of the helicity amplitudes and can be easily derived using the representation (2.11). (See remarks at the end of Sec.2).

The antiquark correlation density matrices $(H_\alpha^{JJ'})_{\lambda_{\bar q}\lambda'_{\bar q}}$ can be obtained from (3.7) by simply replacing $\sigma_3 \to -\sigma_3$ since quark and antiquark helicities are correlated in the simple manner described above.

Inserting the correlation density matrices (3.7) into the differential distribution (2.2) one gets the most general differential distribution including quark polarization. We shall not discuss the general case here but consider as an application the polar angle distribution obtained after integrating out the azimuthal φ and χ dependencies. It is clear that no transverse beam polarization effects remain after these integrations. One obtains for the spin density matrix of the quark

$$\frac{128\pi^2}{\sigma_{pt}}\frac{d\varrho^{(q)}_{\lambda_q\lambda'_q}}{dx_1dx_2d\cos\theta} = \left(G_{A1}\mathbb{1} + G_{A4}\sigma_3\right)\left[\tfrac{3}{8}(1+\cos^2\theta)\sigma_U^{VV} + \tfrac{3}{4}\sin^2\theta\,\sigma_L^{VV}\right] + \left(G_{D4}\mathbb{1} + G_{D1}\sigma_3\right)\tfrac{3}{4}\cos\theta\;\sigma_7^{VA}, \tag{3.8}$$

*Transverse quark (antiquark) polarization components are present even in the quark mass zero limit if the double quark-antiquark density matrix is considered. The transverse polarization components of the quark and antiquark are correlated, as illustrated by the corresponding expression for the transverse polarization components of the lepton tensors in (2.7).

where $\sigma_{pt} = 4\pi\alpha^2/3s$ and [5]

$$G_{A\tau} = (1-h^-h^+)g_{1\tau} + (h^- - h^+)g_{4\tau}\,,$$
$$G_{D\tau} = (1-h^-h^+)g_{4\tau} + (h^- - h^+)g_{1\tau}\,, \qquad \tau = 1,4 \tag{3.9}$$

with the (flavour dependent) electro-weak coupling coefficients $g_{r'r}$ given in (2.3). The degree of longitudinal polarization P_z^q of the quark is obtained from (3.8) by calculating the ratio $\mathrm{Tr}(\rho\sigma_3)/\mathrm{Tr}\rho$. Any of the three* coordinate systems (3.2) with their respective σ_α's could be used to define the polar angle distribution (3.8). In practise one would presumably use the polar angle distribution of the particle whose polarization is measured, i.e. the quark in the application of (3.8), with $\sigma_\alpha = \sigma_\alpha(I)$ and θ the angle between the quark and the electron beam.

The polar angle distribution of the normal to the event plane can be easily obtained by making in (3.8) the substitutions $\sigma_\alpha \to \bar\sigma_\alpha$ and $\theta \to \bar\theta$, where $\bar\sigma_\alpha$ is given by (2.17) in terms of σ_α and $\bar\theta$ is now the angle between the electron beam and the normal to the event plane. From (2.17) and $2\sigma_T = \sigma_L$ and $\sigma_9 = 0$ we find $\bar\sigma_U = \bar\sigma_L = \frac{1}{2}(\sigma_U + \sigma_L)$ and $\bar\sigma_7 = 0$, so that the $\bar\theta$-distribution of the quark density matrix becomes

$$\frac{128\pi^2}{\sigma_{pt}}\frac{d\bar\varrho^{(q)}_{\lambda_q\lambda'_q}}{dx_1dx_2d\cos\bar\theta} = \left(G_{A1}\mathbb{1} + G_{A4}\sigma_3\right)\tfrac{3}{16}(2+\sin^2\bar\theta)\left(\sigma_U^{VV}+\sigma_L^{VV}\right). \tag{3.10}$$

There is no $\cos\bar\theta$-term and the degree of longitudinal quark polarization is now $\bar P_z^q = G_{A4}/G_{A1}$, independent of $\bar\theta$. The same polarization results from (3.8) after integration over $\cos\theta$.

The density matrix θ-distribution of the antiquark has the form (3.8) with σ_3 and $\cos\theta$ replaced by $(-\sigma_3)$ and $(-\cos\theta)$, respectively. This then leads to the relation $\bar P_z^q(\cos\theta) = -P_z^q(-\cos\theta)$ between the longitudinal polarization of the antiquark and quark. Identical results have been obtained in [11] using the covariant "trace" method.

*) Since we have integrated over χ the difference between systems (a) and (b) has been lost.

Proposals for the measurement of the quark's longitudinal polarization are based on the presumption that the quark's helicity is handed down to fast fragmentation products near $x = 1$ ($x = 2E/\sqrt{q^2}$) [11,12]. If the (fast) fragmentation products have spin and decay weakly (as e.g. the Λ-particle) the longitudinal polarization of the particle and hopefully of the quark can be reconstructed. The proposed mechanisms have not as yet been subjected to experimental tests, but, given enough statistics, the polarization tests should be feasible and provide an additional test of the underlying quark dynamics. Another proposal is to look for parity-odd correlations among the fastest particles of the jet [13].

c) Gluon density matrix

As a next step we calculate the gluon spin density matrix. It has more structure than the quark spin density matrix. In particular there are now off-diagonal components related to linearly polarized gluons. One has in general

$$\left(H_\alpha\right)_{\lambda_g\lambda_g'} = \frac{1}{2}\left(\sigma_\alpha \mathbb{1} + \rho_{\alpha x}\sigma_1 + \rho_{\alpha y}\sigma_2 + \rho_{\alpha z}\sigma_3\right), \tag{3.11}$$

where σ_α are the unpolarized (hadronic) correlation cross sections introduced before and $\vec{\rho}_\alpha = (\rho_{\alpha x}, \rho_{\alpha y}, \rho_{\alpha z})$ are the correlation Stokes vectors of the gluon with components referring to the event coordinate system Oxyz.

In Table 3 we list the various gluon density matrix components for system IIIa which, as a reminder, has the gluon momentum in the z-direction. The unpolarized correlation cross sections σ_α are not explicitly given since they already appear in Table 2. Instead we list only their symmetry

property under $x_1 \leftrightarrow x_2$. The parity classification of the components $\rho_{\alpha x}$ is the same as for the cross sections σ_α discussed at the end of Sec.2, whereas the components $\rho_{\alpha y}$ and $\rho_{\alpha z}$ show the opposite parity classification. Again, zero contributions resulting from parity have been denoted by dashes in Table 3. Zero contributions resulting from the reality of the underlying Born term process are indicated by '0'*), whereas zeros due to charge conjugation are indicated by 'zero'.

The $x_1 \leftrightarrow x_2$ symmetry pattern of the entries in Table 3 can be worked out from the quark-antiquark exchange relations (3.6). For α = U,L,T,4,7 (transverse-transverse and longitudinal-longitudinal parts) the parity conserving VV-contributions are symmetric under $x_1 \leftrightarrow x_2$ and the parity violating VA-contributions are antisymmetric. The opposite holds true for the longitudinal-transverse interference terms α = 5,I,8,9.

The density matrix components in Table 3 allow one to write down the most general multidifferential gluon density matrix angular distribution as given by (2.2) and (2.14). We shall limit our discussion to the (θ,χ)-distribution. The dependence on transverse beam polarization effects drops out after the azimuthal ω-integration and one obtains

$$\frac{128\pi^3}{\sigma_{pt}}\frac{d\rho^{(g)}_{\lambda_g\lambda_g'}}{dx_1\,dx_2\,d\cos\theta\,d\chi} = \frac{1}{2}\left(A\,\mathbb{1} + B_x\sigma_1 + B_y\sigma_2 + B_z\sigma_3\right), \tag{3.12}$$

where

*) These components are zero even to order $O(\alpha_s^2)$ as shown explicitly for σ_9^{VV} in [8] and argued for in more detail for the cross section components at the end of Sec.2.

$$A = G_{A1}\left[\frac{3}{8}(1+\cos^2\theta)\,\sigma_U^{VV} + \frac{3}{4}\sin^2\theta\,\sigma_L^{VV} + \frac{3}{4}\sin^2\theta\cos 2\chi\,\sigma_T^{VV} - \frac{3}{2\sqrt{2}}\sin 2\theta\cos\chi\,\sigma_I^{VV}\right] + G_{D4}\left[\frac{3}{4}\cos\theta\,\sigma_7^{VA} - \frac{3}{\sqrt{2}}\sin\theta\cos\chi\,\sigma_8^{VA}\right],$$

$$B_x = G_{A1}\left[\frac{3}{8}(1+\cos^2\theta)\,\rho_{Ux}^{VV} + \frac{3}{4}\sin^2\theta\,\rho_{Lx}^{VV} + \frac{3}{4}\sin^2\theta\cos 2\chi\,\rho_{Tx}^{VV} - \frac{3}{2\sqrt{2}}\sin 2\theta\cos\chi\,\rho_{Ix}^{VV}\right] + G_{D4}\left[\frac{3}{4}\cos\theta\,\rho_{7x}^{VA} - \frac{3}{\sqrt{2}}\sin\theta\cos\chi\,\rho_{8x}^{VA}\right],$$

$$B_y = G_{A1}\left[-\frac{3}{4}\sin^2\theta\sin 2\chi\,\rho_{4y}^{VV} + \frac{3}{2\sqrt{2}}\sin 2\theta\sin\chi\,\rho_{5y}^{VV}\right] + G_{D4}\left[\frac{3}{\sqrt{2}}\sin\theta\sin\chi\,\rho_{9y}^{VA}\right],$$

$$B_z = G_{D1}\left[\frac{3}{4}\cos\theta\,\rho_{7z}^{VV} - \frac{3}{\sqrt{2}}\sin\theta\cos\chi\,\rho_{8z}^{VV}\right] + G_{A4}\left[\frac{3}{8}(1+\cos^2\theta)\,\rho_{Uz}^{VA} - \frac{3}{2\sqrt{2}}\sin 2\theta\cos\chi\,\rho_{Iz}^{VA}\right], \qquad (3.13)$$

and where the electro-weak coupling coefficients G_{Ar} and G_{Dr} are defined in (3.9). The correlation cross sections σ_α and the correlation Stokes vectors $\vec{\rho}_\alpha$ are given, for the event frame IIIa (3.2), in Table 2 and 3, respectively. One notes the different angular dependence of the unpolarized and linear polarized cross section contributions σ_α and $\rho_{\alpha x}$, $\rho_{\alpha y}$ on the one hand and of the circular polarization contribution $\rho_{\alpha z}$ on the other hand under the parity transformation $\theta \to \pi - \theta$, $\chi \to \pi + \chi$. In the former case the VV(VA)-parts multiply the even (odd) angular terms, whereas the opposite behaviour holds true for the circular polarization term.

The Stokes vector of the gluon has the components $(B_x/A, B_y/A, B_z/A)$ with respect to the event frame IIIa. Thus B_x/A (B_y/A) measure the normalized cross section differences for gluons linearly polarized out and in of the event plane (of the x = y plane), whereas B_z/A measures the corresponding difference for right (positive helicity) and left (negative helicity) circularly polarized gluons. The (maximal) linear gluon polarization vector is rotated out of the event plane by an angle $\psi = \frac{1}{2}\,\mathrm{arctg}(B_y/B_x)$. However, after χ-integration, $B_y = 0$ so that $\psi = 0^\circ$ or 90° depending on whether $B_x < 0$ or $B_x > 0$. The latter two cases correspond to the (maximal) linear polarization of the gluon being in or perpendicular to the event plane.

The expressions (3.13) considerably simplify if the quark and antiquark jets are not distinguished. In this case we have to add the contributions

$$\sigma_\alpha(\mathrm{IIIa};\ x_1 = x,\ x_2 = y) + \sigma_\alpha(\mathrm{IIIb};\ x_1 = y,\ x_2 = x) \equiv \sigma_\alpha(\mathrm{III};\ x,y) \qquad (3.14)$$

for $x > y$, and similarly for $\vec{\rho}_\alpha$. From Table 2 and 3 it then follows that the VA-contributions going with G_{D4} and G_{A4} in (3.13) drop out in (3.14). As a result the linear polarization of the gluon becomes independent of energy, longitudinal beam polarization and neutral current effects. Only the circular polarization continues to depend on these effects through the factor G_{D1}/G_{A1}; it vanishes, however, after θ-integration.

In (3.12) and (3.13) the linear polarization of the gluon is specified relative to the event plane. This, however, is not always convenient. For example, it would be easier to measure the gluon's linear polarization relative to the gluon-beam axis plane, since such a measurement does not require the determination of the event plane. By inspection of Fig.2 it follows that for system III a rotation by $(-\chi)$ around the gluon's direction (Oz) brings the event plane (Oxz) into the gluon-beam axis plane (Oz'z). Under such a rotation the unpolarized cross section (A) and the circular component (B_z) of the Stokes vector remain unchanged, whereas the linear components (B_x, B_y) trans-

form according to (B.3). After integrating over χ one obtains for the new density matrix polar angle distribution

$$\frac{64\pi^2}{\sigma_{pt}}\,\frac{d\,\tilde{\varrho}^{(g)}_{\lambda_g\lambda'_g}}{dx_1\,dx_2\,d\cos\theta} = \frac{1}{2}\left(\tilde{A}\,\mathbb{1} + \tilde{B}_x\,\sigma_1 + \tilde{B}_z\,\sigma_3\right), \qquad (3.15)$$

where

$$\tilde{A} = G_{A1}\left[\tfrac{3}{8}(1+\cos^2\theta)\,\sigma_U^{VV} + \tfrac{3}{4}\sin^2\theta\,\sigma_L^{VV}\right] + G_{D4}\left[\tfrac{3}{4}\cos\theta\,\sigma_7^{VA}\right],$$

$$\tilde{B}_x = G_{A1}\left[\tfrac{3}{8}\sin^2\theta\,(\varrho_{Tx}^{VV} + \varrho_{4y}^{VV})\right],$$

$$\tilde{B}_z = G_{D1}\left[\tfrac{3}{4}\cos\theta\,\varrho_{7z}^{VV}\right] + G_{A4}\left[\tfrac{3}{8}(1+\cos^2\theta)\,\varrho_{Uz}^{VA}\right]. \qquad (3.16)$$

In order to compare to the linear polarization relative to the event plane as obtained from (3.13), we consider the angle integrated case. One obtains ($\varrho_{Tx}^{VV} + \varrho_{4y}^{VV} = 2(H_{+-})_{+-}$).

$$\tilde{P}_{lin}(x_1,x_2) = \frac{d\tilde{\sigma}_\parallel - d\tilde{\sigma}_\perp}{d\tilde{\sigma}_\parallel + d\tilde{\sigma}_\perp} = \frac{-\frac{1}{2}(\varrho_{Tx}^{VV}+\varrho_{4y}^{VV})}{\sigma_U^{VV}+\sigma_L^{VV}} = \frac{(1-x_1)(1-x_2)}{x_3^2\,(x_1^2+x_2^2)}\,, \qquad (3.17)$$

to be compared with [14]*)

$$P_{lin}(x_1,x_2) = \frac{d\sigma_\parallel - d\sigma_\perp}{d\sigma_\parallel + d\sigma_\perp} = \frac{-(\varrho_{Ux}^{VV}+\varrho_{Lx}^{VV})}{\sigma_U^{VV}+\sigma_L^{VV}} = \frac{2(1-x_3)}{x_1^2+x_2^2} \qquad (3.18)$$

for the linear gluon polarization relative to the event plane. In both cases the gluon's (maximal) linear polarization is in the respective plane and does not depend on beam polarization and/or neutral current effects. The circular polarization, however, depends on this effects as

$$P_{circ}(x_1,x_2) = \frac{d\sigma_+ - d\sigma_-}{d\sigma_+ + d\sigma_-} = \frac{G_{A4}}{G_{A1}}\,\frac{\varrho_{Uz}^{VA}}{\sigma_U^{VV}+\sigma_L^{VV}} = -\frac{G_{A4}}{G_{A1}}\,\frac{x_1^2-x_2^2}{x_1^2+x_2^2} \qquad (3.19)$$

*)After completion of this work we learned that gluon polarization in $e^+e^- \to \gamma,Z^0 \to q\bar{q}g$ has been considered recently also in [32].

in both cases. If the quark and antiquark jets are not distinguished the angle-integrated circular polarization (3.19) vanishes. The linear polarizations (3.17) and (3.18), however, survive.

As a last application and further illustration we extend the calculation of [15] where the polar angle dependence of the linear gluon polarization was calculated for the transversity polar angle $\bar{\theta}$ between the electron beam and the normal to the event plane. We generalize the result of [15] by including beam polarization and parity violating effects.

Referring to (2.17) for the necessary transformations to the transversity frame one finds

$$\frac{64\pi^2}{\sigma_{pt}}\,\frac{d\,\bar{\varrho}^{(g)}_{\lambda_g\lambda'_g}}{dx_1\,dx_2\,d\cos\bar{\theta}} = \frac{1}{2}\left(\bar{A}\,\mathbb{1} + \bar{B}_x\,\sigma_1 + \bar{B}_y\,\sigma_2 + \bar{B}_z\,\sigma_3\right), \qquad (3.20)$$

where

$$\bar{A} = G_{A1}\left[\tfrac{3}{16}\,(2+\sin^2\bar{\theta})\,(\sigma_U^{VV}+\sigma_L^{VV})\right],$$

$$\bar{B}_x = G_{A1}\left[\tfrac{3}{8}(1+\cos^2\bar{\theta})\left(\tfrac{1}{2}\varrho_{Ux}^{VV} + \varrho_{Lx}^{VV} - \varrho_{Tx}^{VV}\right) + \tfrac{3}{4}\sin^2\bar{\theta}\left(\tfrac{1}{2}\varrho_{Ux}^{VV} + \varrho_{Tx}^{VV}\right)\right],$$

$$\bar{B}_y = G_{D4}\left[\frac{3}{\sqrt{2}}\cos\bar{\theta}\;\varrho_{9y}^{VA}\right],$$

$$\bar{B}_z = G_{A4}\left[\tfrac{3}{16}\,(2+\sin^2\bar{\theta})\,\varrho_{Uz}^{VA}\right]. \qquad (3.21)$$

The (maximal) linear polarization of the gluon is rotated out of the event plane by an angle $\psi = \frac{1}{2}\,\mathrm{arctg}\,(\bar{B}_y/\bar{B}_x)$. Except for the $\bar{B}_y$-contribution which is odd under $\bar{\theta} \to \bar{\theta} - \pi$, all other contributions $\bar{A}$, $\bar{B}_x$ and $\bar{B}_z$ are even.

In the purely electromagnetic case where $G_{D4} = G_{A4} = 0$ and $G_{A1} = Q_q^2$ one recovers the result of [15]. Upon $\bar{\theta}$-integration one recovers the result of [14], as would be true for (3.13) after integration over θ and χ. Some suggestions of how to measure the gluon's polarization can be found in [14] and [16].

4. $e^+e^- \to Q\bar{Q}(1^{--}) \to ggg(\gamma\, gg)$

The next expected onium resonance, the toponium, may be heavy enough to be sensitive to γ-Z^0 interference effects in its production. Although excited only by hadronic vector currents, parity violating effects enter through the lepton vertex. In this section we work out the production and three-gluon decay of a heavy (1^{--}) quarkonium state in the presence of parity violating and beam polarization effects.

The calculation of the decay of a heavy quarkonium state into three vector gluons proceeds in complete analogy to the corresponding positronium decay calculation. Figure 3 illustrates the process. In the nonrelativistic approximation, and neglecting binding energies, one has $M \cong 2m$ and $P = p - \bar{p} \cong 2p$, where M and m are the masses of the quarkonium state and its heavy quark constituent, respectively. For the spin projection of the quarkonium state, it is convenient to use the covariant form $\not\epsilon(\not P - M) \cong 2\not\epsilon(\not p - m)$, which is well known from relativistic SU(6) calculations [17]. The amplitude is then given by the covariant trace

$$M_{ijk} = N_{ijk}\Big\{ 2m\,\mathrm{Tr}\big[\not\epsilon(\not p - m)\not e_3^*(-\not p + \not p_3 - m)^{-1}\not e_2^*(\not p - \not p_1 - m)^{-1}\not e_1^*\big] + \text{cyclic perm. } (1,2,3)\Big\} \tag{4.1}$$

All constants have been absorbed into

$$N_{ijk} = \tfrac{1}{2} d_{ijk} (\alpha_s 4\pi)^{3/2} N\,,$$

$$N = 2\sqrt{\tfrac{2}{3}}\,\Psi(0)\, m^{-3/2}\,, \tag{4.2}$$

where d_{ijk} is the symmetric colour coupling coefficient, $\Psi(0)$ is the wave function evaluated at the origin and α_s is the strong

QCD coupling constant. e and e_i are the polarization 4-vectors of the 1^{--}-quarkonium state and of the threevector gluons, respectively.

The corresponding matrix element for the γ-inclusive process $Q\bar{Q}(1^{--}) \to \gamma gg$ is given by the same expression (4.1) but with N_{ijk} replaced by

$$N_{ij} = \delta_{ij}\sqrt{\alpha}\,\alpha_s (4\pi)^{3/2} Q_q^2 N\,. \tag{4.2'}$$

The trace in (4.1) can be easily computed by taking advantage of the relations valid in the nonrelativistic approximation in the c.m. system $p\cdot e_1 = p\cdot e = 0$ [18].

In order to calculate helicity amplitudes we need to specify a coordinate system. For this purpose we divide the phase space into six equivalent regions according to the six possible energy orderings $x_i \geqslant x_j \geqslant x_k$. The x_i are the conventional scaled energies $x_i = E_i/\frac{1}{2}M \cong E_i/m$ such that $x_1+x_2+x_3 = 2$. Our coordinate system is (arbitrarily) chosen such that with the energy ordering $x_1 \geqslant x_2 \geqslant x_3$ $\vec{p}_1$ is along the z-axis and $\vec{p}_2$ in the (pos.x;z) half plane. In the γ-inclusive case we always choose p_γ along the z-axis and assign $x_1 = x_\gamma$ for $0 \leq x_\gamma \leq 1$, and $x_2 \geq x_3$ with $\vec{p}_2$ in the (pos.x; z) half-plane. This means that we do not include a statistics factor 1/6 (1/2 in the γ-inclusive case) in the following cross-section formulas as would be appropriate if all of phase space were taken.

From spin counting there are twelve helicity amplitudes after using parity, designated as $F_{\lambda_1\lambda_2\lambda_3;\lambda_{Q\bar{Q}}}$. Using the helicity representation of the gluon polarization vectors given in Appendix A, and $e_\pm^\mu = \mp(2)^{-1/2}(0;1,\pm i,0)$ and $e_0^\mu = (0;0,0,1)$ for the $Q\bar{Q}(1^{--})$ polarization vector according to (A.6), the helicity amplitudes can be evaluated from the amplitude (4.1). They are given in Table 4.

Since we are dealing with identical gluons, Bose symmetry imposes the following relations on the helicity amplitudes

$$F_{\lambda_1\alpha\beta;\,\pm 0}(x_1,x_2,x_3) = \pm F_{\lambda_1\beta\alpha;\,\pm 0}(x_1,x_3,x_2) \qquad (4.3)$$

which can be seen to hold true for the helicity amplitudes in Table 4. The ($\pm$) signs in (4.3) result from having to rotate the event system by 180° around the z-axis when exchanging $x_2 \leftrightarrow x_3$ according to our convention that the second most energetic gluon lies in the (pos.x,z) half plane. Corresponding sign changes occur in the $e^+e^- \to q\bar{q}g$ helicity amplitudes when going from systems a to b (see caption of Table 2). The remaining twelve (dependent) helicity amplitudes may be obtained from the parity relations

$$F_{-\lambda_1-\lambda_2-\lambda_3;\,\bar{0}} = \pm F_{\lambda_1\lambda_2\lambda_3;\,\pm 0} \qquad (4.4)$$

Since the $Q\bar{Q}(1^{--})$ quarkonium state can only be excited by vector currents, there are correspondingly no axial vector current helicity amplitudes. Accordingly the hadronic tensors have less structure than in the case $e^+e^- \to q\bar{q}g$. In explicit terms, only $H^1_{\mu\nu} = H^2_{\mu\nu}$ are nonzero in the notation of (2.1). This observation leads to a simplification of the general differential rate formula $\propto g_{ij} L^{i}_{\mu\nu} H^{j}_{\mu\nu}$ since only the combinations $g_{i1}+g_{i2} = 2g_{i1}(a_f=0)$ enter (the axial vector coupling to the hadronic final state a_f drops out in this combination, as can be seen from (2.3)). Therefore the differential rate acquires a factorized form in the electro-weak coupling indices, i.e. the differential rate is proportional to $g_{i1}(a_f=0)\, L^{i}_{\mu\nu} \cdot 2H^{1}_{\mu\nu}$ on the (1^{--}) quarkonium resonance. In the following we shall use this reduced

form and refer to the vector current hadronic tensor as $H_{\mu\nu} \equiv H^{VV}_{\mu\nu} = 2H^{1}_{\mu\nu}$. In Table 5 we have listed the independent components of the single gluon correlation density matrix $(H_{\mu\nu})_{\lambda_1\lambda_1'}$ of the most energetic gluon.

We shall write the full differential rate in a form where the part related to the production of the heavy quarkonium resonance has been factored out. The production mechanism enters insofar as the decaying heavy quarkonium state is polarized as specified by the e^+e^--production mechanism. Thus the differential single-gluon density matrix is written as

$$\frac{d\,\varrho_{\lambda_1\lambda_1'}}{dx_1dx_2d\varphi d\chi d\cos\Theta} = \frac{1}{2\pi}\frac{m}{4(4\pi)^4}\frac{g_{i1}(a_f=0)}{G_{A1}(a_f=0)} L^{i}_{\mu\nu}(H_{\mu\nu})_{\lambda_1\lambda_1'} \qquad (4.5)$$

where $G_{A1}(a_f = 0)$ has been defined in (3.9). The density matrix (4.5) is normalized to the total $Q\bar{Q}(1^{--})$ decay rate

$$\Gamma_{Q\bar{Q}(1^{--})\to ggg} = \frac{40}{81}\alpha_s^3(\pi^2-9)\frac{|\Psi(0)|^2}{m^2} \qquad (4.6)$$

In Table 5 we list the relevant density matrix components, where zero contributions are denoted as in Table 3. The entries in Table 5 are symmetric under $x_2 \leftrightarrow x_3$ for the transverse-transverse and longitudinal-longitudinal parts α = U,L,T,4,7 and antisymmetric for the transverse-longitudinal parts α = 5,I,8,9 due to Bose symmetry as can be worked out from the relations (4.3).

As in the case $e^+e^- \to q\bar{q}g$ discussed in Section 3, formula (4.5) allows one to write down the most general one-gluon density matrix distribution in the presence of p.v. interactions and longitudinal and transverse beam polarization. We shall limit our discussion to the φ-integrated form of (4.5), i.e. transverse beam polarization effects are integrated out. One has

$$\frac{d\varrho_{\lambda_1\lambda_1'}}{dx_1 dx_2 d\chi d\cos\Theta} = \frac{1}{6}\frac{m}{(4\pi)^4}\left(A\mathbb{1} + B_x\sigma_1 + B_y\sigma_2 + B_z\sigma_3\right) \tag{4.7}$$

where

$$\begin{aligned}
A &= \left[\tfrac{3}{8}(1+\cos^2\Theta)\sigma_U + \tfrac{3}{4}\sin^2\Theta\,\sigma_L + \tfrac{3}{4}\sin^2\Theta\cos 2\chi\,\sigma_T - \tfrac{3}{2\sqrt{2}}\sin 2\Theta\cos\chi\,\sigma_I\right]\\
B_x &= \left[\tfrac{3}{8}(1+\cos^2\Theta)\varrho_{Ux} + \tfrac{3}{4}\sin^2\Theta\,\varrho_{Lx} + \tfrac{3}{4}\sin^2\Theta\cos 2\chi\,\varrho_{Tx} - \tfrac{3}{2\sqrt{2}}\sin 2\Theta\cos\chi\,\varrho_{Ix}\right]\\
B_y &= \left[-\tfrac{3}{4}\sin^2\Theta\sin 2\chi\,\varrho_{4y} + \tfrac{3}{2\sqrt{2}}\sin 2\Theta\sin\chi\,\varrho_{5y}\right]\\
B_z &= \frac{G_{D1}(a_f=0)}{G_{A1}(a_f=0)}\left[\tfrac{3}{4}\cos\Theta\,\varrho_{7z} - \tfrac{3}{\sqrt{2}}\sin\Theta\cos\chi\,\varrho_{8z}\right]
\end{aligned} \tag{4.8}$$

with G_{A1} and G_{D1} defined in (3.9) and σ_α, $\vec{\rho}_\alpha$ given in Table 5.

The produced gluon (or photon in the Υ -inclusive case) is polarized both linearly and circularly as B_x, B_y and B_z are unequal zero. The degree of linear and circular polarization is given by $(B_x^2 + B_y^2)^{1/2}/A$ and B_z/A, and the maximal linear polarization is rotated out of the decay plane by an angle $\psi = \mathrm{arctg}(B_y/B_x)$. Compared to the purely electromagnetic case with no longitudinal beam polarization, the p.v. lepton interactions do not affect the unpolarized and linearly polarized gluon distribution components, but induce new angular structure through the circular polarization component.

The density matrix distribution (4.7) - (4.8) can be formally obtained (up to a normalization factor) from (3.12) - (3.13) by setting G_{A4} and G_{D4} to zero, replacing G_{A1} and G_{D1} by $G_{A1}(a_f = 0)$ and $G_{D1}(a_f = 0)$, and σ_α^{VV} and $\vec{\rho}_\alpha^{VV}$ by σ_α and $\vec{\rho}_\alpha$ from Table 5. This "substitution rule" also allows one to obtain from (3.15) - (3.16) the density matrix polar angle distribution of the gluon (or photon) with the components $\tilde{B}_x$ ($\tilde{B}_y$) of the Stokes vector referring to directions in (perpendicular to) the gluon (or photon) -beam axis plane. This is particularly interesting in the Υ-inclusive case, since a measurement of the linear polarization of the photon relative to the photon-beam axis plane does not involve any hadron event specification with its accompanying uncertainties. In the angle integrated case we obtain from (3.17) - (3.18) for the linear polarization of the photon:

$$\tilde{P}_{lin}(x_1,x_2) = \frac{-\frac{1}{2}(\varrho_{Tx}+\varrho_{4y})}{\sigma_U+\sigma_L} = \frac{-(1-x_2)^2(1-x_3)^2}{x_1^2\left[x_1^2(1-x_1)^2 + x_2^2(1-x_2)^2 + x_3^2(1-x_3)^2\right]} \tag{4.9}$$

with respect to the photon-beam axis plane, and

$$P_{lin}(x_1,x_2) = \frac{-(\varrho_{Ux}+\varrho_{Lx})}{\sigma_U+\sigma_L} = \frac{-2(1-x_1)(1-x_2)(1-x_3)}{x_1^2(1-x_1)^2 + x_2^2(1-x_2)^2 + x_3^2(1-x_3)^2} \tag{4.10}$$

with respect to the event plane. Since P_{lin} and $\tilde{P}_{lin}$ are both negative, the maximal linear polarization of the photon (or gluon) is normal to the corresponding (x,z)-plane, i.e. to the event plane in case (4.10) and to the photon-beam axis plane in case (4.9). Regarding the angle integrated circular polarization of the photon it vanishes in both cases.

The polar angle distribution of the normal to the event plane can easily be obtained (up to normalization) from (3.21) by using the "substitution rule" stated above, i.e. by setting $G_{A4} = G_{D4} = 0$ and replacing G_{A1} by $G_{A1}(a_f = 0)$. It is noteworthy that the simple form of the polar $\bar{\theta}$-distribution in (3.21)

due to the relation $\sigma_L = 2\sigma_T$ holds true also in the heavy quarkonium decay case since one has the same relation here too. The Stokes vector now becomes $(\overline{B}_x/\overline{A}, 0, 0)$ so that there is no circular, but only a linear polarization of the photon (gluon) in the $\overline{\theta}$-distribution.

The unpolarized cross section distributions contained in (4.7) agree with the calculation of Koller and Walsh [4]. Parts of the polarization content of (4.7) have been presented in [16] and in [18] which includes also some comments on the (difficult) task of measuring the photon's polarization in the γ-inclusive decay of a heavy $Q\bar{Q}(1^{--})$ state. Suggestions for measuring the gluon's linear polarization can be found in [14,15,16]. An interesting application of the helicity method can be found in [19] where the density matrix of the $J^{PC} = 2^{++}$ f^o-meson produced in $e^+e^- \to Q\bar{Q}(1^{--}) \to \gamma f^o$ was calculated using as dynamical input the $gg \to f^o$ fusion mechanism. The results of this calculation are in good agreement with experiment [20].

5. Concluding Remarks

In considering the $q\bar{q}g$-production case in Sec.3 we have limited our discussion to mass zero quarks. Mass effects can easily be included by using massive helicity spinors. The number of independent helicity amplitudes is doubled to twelve. Quark and antiquark helicities are no longer correlated in a simple manner leading to the appearance of transverse quark polarization components. The relations between the p.c. and p.v. helicity amplitudes F^V and F^A are more complex due to mass effects, and thus, one has in general $H^{VV}_{\mu\nu} \neq H^{AA}_{\mu\nu}$ and $H^{VA}_{\mu\nu} \neq H^{AV}_{\mu\nu}$. This means that in general all $H^r_{\mu\nu}$ (r= 1,...4) contribute which leads to more structure in the predicted beam-event correlations. Also, the simple factorizing structure of the diagonal quark spin density matrix (3.7) does not hold in the massive quark case. The T-odd correlation cross sections and density matrix elements which are zero in the mass zero case even at the one-loop level [8] acquire nonzero values at the one-loop level in the massive case [21].

Similarly, off-mass-shell or effective massive gluons can be treated within the helicity formalism by including an additional longitudinal degree of freedom for the gluon.

The helicity formalism as developed in this paper is also well suited for a discussion of cross section and polarization phenomena in two-particle production processes, as e.g. $e^+e^- \to q\bar{q}$, $\ell\bar{\ell}$ and $e^+e^- \to Q\bar{Q}(1^{--}) \to \ell\bar{\ell}$, $q\bar{q}$ [22]. As an example, we have derived in Sect.2 the structure of the lepton tensors $L^r_{\mu\nu}$ by using the helicity method.

Three-body decays of heavy quarkonium states with different J^{PC} quantum numbers have been recently discussed within the helicity method in [23].

It would also be desirable to have available the helicity amplitudes for the four-body processes $e^+e^- \to q\bar{q}gg(q\bar{q}q\bar{q})$ and $e^+e^- \to Q\bar{Q}(1^{--}) \to gggg(gg\bar{q}q)$ as these will become an important area of experimental and theoretical study in the coming years. Although the processes $e^+e^- \to q\bar{q}gg(q\bar{q}q\bar{q})$ have been studied in some detail using the "trace" method [24], a helicity treatment can be expected to be more efficient and physically transparent as we hope to have examplified by the calculations in this paper.

Acknowledgement

We would like to thank D.McKay,G.Kramer,G.Schierholz and D.Wähner for discussions and a critical reading of the manuscript.

Appendix A: Helicity spinors and polarization vectors.

For the Dirac bispinors of the leptons and quarks it is convenient to use the chirality (or Weyl) representation (γ_5 diagonal), which reduces to a two-component form in the high energy (or mass zero) limit considered in this paper. In the chirality representation the γ-matrices are given by

$$\gamma^0 = \begin{pmatrix} 0 & \mathbb{1} \\ \mathbb{1} & 0 \end{pmatrix}, \quad \vec{\gamma} = \begin{pmatrix} 0 & \vec{\sigma} \\ -\vec{\sigma} & 0 \end{pmatrix}, \quad \gamma_5 = \begin{pmatrix} -\mathbb{1} & 0 \\ 0 & \mathbb{1} \end{pmatrix}, \tag{A.1}$$

with the 2 x 2 unit and Pauli matrices

$$\mathbb{1} = \begin{pmatrix} 1 & 0 \\ 0 & 1 \end{pmatrix}, \quad \sigma_1 = \begin{pmatrix} 0 & 1 \\ 1 & 0 \end{pmatrix}, \quad \sigma_2 = \begin{pmatrix} 0 & -i \\ i & 0 \end{pmatrix}, \quad \sigma_3 = \begin{pmatrix} 1 & 0 \\ 0 & -1 \end{pmatrix}. \tag{A.2}$$

One has $\gamma^\mu \gamma^\nu + \gamma^\nu \gamma^\mu = 2g^{\mu\nu}$, where $g^{\mu\nu} = g_{\mu\nu} = \mathrm{diag}(1; -1, -1, -1)$ is the metric tensor. Writing the momentum vector (for high energy fermions) as

$$p^\mu \approx E(1; \vec{n}), \quad \vec{n} = \vec{p}/|\vec{p}| = (\sin\theta\cos\varphi, \sin\theta\sin\varphi, \cos\theta), \tag{A.3}$$

we find for the helicity bispinors (in the representation (A.1))

$$u_+(p) = \sqrt{2E}\begin{pmatrix} 0 \\ w_+(\vec{n}) \end{pmatrix}, \qquad u_-(p) = \sqrt{2E}\begin{pmatrix} w_-(\vec{n}) \\ 0 \end{pmatrix},$$

$$v_+(p) = \sqrt{2E}\begin{pmatrix} -w_-(\vec{n}) \\ 0 \end{pmatrix}, \qquad v_-(p) = \sqrt{2E}\begin{pmatrix} 0 \\ -w_+(\vec{n}) \end{pmatrix}, \tag{A.4}$$

where $u_\pm(v_\pm)$ describe a fermion (antifermion) of helicity $\lambda = \pm 1/2$. The two-component spinors $w_\pm(\vec{n})$ are normalized eigenvectors of $\vec{n}\cdot\vec{\sigma}$ with eigenvalues ± 1, given explicitly by

$$w_\pm(\vec{n}) = [2(1+n_z)]^{-1/2}\left(\mathbb{1} \pm \vec{n}\cdot\vec{\sigma}\right)\xi_\pm = \sum_{\lambda=\pm\frac{1}{2}} D^{1/2}_{\lambda,\pm\frac{1}{2}}(\varphi,\theta,-\varphi)\,\xi_{2\lambda}\,, \tag{A.5}$$

where $\xi_+ = (1\ 0)^T$, $\xi_- = (0\ 1)^T$ are the eigenvectors of σ_z and $D^{1/2}_{\lambda,\lambda'}(\varphi,\theta,-\varphi)$ is the Wigner rotation matrix for spin 1/2 and Euler angles $\varphi, \theta, -\varphi$. This choice of the Euler angles corresponds to the phase conventions of Jacob and Wick [25] as described in [26].*) Defining the spinors $w_\pm(-\vec{n})$ with quantization axis along $\vec{n}' = -\vec{n}$ as having Euler angles $(\pi+\varphi, \pi-\theta, -\pi-\varphi)$, the second form of $w_\pm(\vec{n})$ given in (A.5) is particularly useful for particles moving along the negative z-axis. The bispinors (A.4) are eigenvectors of γ_5:

$$\gamma_5 u_\pm = \pm u_\pm\,, \quad \gamma_5 v_\pm = \mp v_\pm\,, \quad \bar{u}_\pm \gamma_5 = \mp \bar{u}_\pm\,, \quad \bar{v}_\pm \gamma_5 = \pm \bar{v}_\pm \tag{A.6}$$

implying simple relations between vector and axial-vector helicity amplitudes.

For the vector (V_μ) and axial-vactor (A_μ) current operators we define their spherical components by

$$J_\sigma = -\epsilon^\mu_\sigma J_\mu = \vec{\epsilon}_\sigma \cdot \vec{J} \qquad (\sigma = 0, \pm\,; \quad J^\mu = V^\mu, A^\mu)$$
$$J_\pm = \mp\frac{1}{\sqrt{2}}(J_x \pm i J_y)\,, \qquad J_0 = J_z\,, \tag{A.7}$$

where we have used the explicit expressions

$$\epsilon^\mu_\pm = \frac{1}{\sqrt{2}}(0; \mp 1, -i, 0)\,, \qquad \epsilon^\mu_0 = (0; 0, 0, 1) \tag{A.8}$$

for the rest frame polarization vectors of a (massive) spin-one particle (virtual photon or Z^0 in the c.m.s. of the reaction $e^+e^- \to \gamma, Z^0 \to$ final state).

Similarly to (A.5), the polarization vectors of a massless vector particle (real photon or gluon) having helicity $\lambda = \pm 1$ can be expressed through (A.8)

$$\epsilon^\mu_\pm(p) = \sum_{\sigma=0,\pm1} D^1_{\sigma,\pm1}(\varphi,\theta,-\varphi)\,\epsilon^\mu_\sigma \tag{A.9}$$
$$= \frac{1}{\sqrt{2}}\, e^{\pm i\varphi}(0; \mp\cos\theta\cos\varphi + i\sin\varphi, \mp\cos\theta\sin\varphi - i\cos\varphi, \pm\sin\theta)$$

where $D^1_{\sigma,\lambda}$ is the Wigner rotation matrix for spin 1 and θ,φ are the polar and azimuthal angle of the 3-momentum as defined in (A.3).

---

*) Our chirality spinors are transformed to the usual Pauli-Dirac representation (γ_0 diagonal) helicity spinors used in [26] by $\psi_{PD} = A\psi$, $\bar{\psi}_{PD} = \bar{\psi}A^{-1}$, where $A = \frac{1}{\sqrt{2}}\begin{pmatrix} \mathbb{1} & \mathbb{1} \\ -\mathbb{1} & \mathbb{1} \end{pmatrix}$, $A^{-1} = A^+ = A^T$ and $\bar{\psi} = \psi^+\gamma_0$ ($\psi = u_\pm, v_\pm$). Correspondingly we have $\gamma^\mu_{PD} = A\gamma^\mu A^{-1}$.

Appendix B: Density Matrix Description of Photon (Gluon)

The normalized density matrix describing the most general statistical mixture of partially polarized photons (or gluons) reads

$$\rho_{\lambda\lambda'} = \frac{1}{2}\left(\mathbb{1} + \xi_x\sigma_1 + \xi_y\sigma_2 + \xi_z\sigma_3\right) \tag{B1}$$

where $\lambda, \lambda' = \pm 1$ denote the two possible helicity configurations of a massless spin one particle. The "vector" $\vec{\xi}$ is referred to as the (helicity basis) Stokes vector *). It has the real components $\xi_i = \mathrm{Tr}(\rho\sigma_i)$. The degree of polarization is given by $P = (\xi_x^2 + \xi_y^2 + \xi_z^2)^{1/2}$, where $0 \leq P \leq 1$. P = 1 corresponds to a pure polarization state, linearly polarized if $\xi_z = 0$, circularly polarized if $\xi_x = \xi_y = 0$ and elliptically polarized in the general case $\xi_z \neq 0$ and $(\xi_x^2 + \xi_y^2) \neq 0$. For partial polarization $P \neq 1$ the same classification applies. $P_{circ} = |\xi_z|$ and $P_{lin} = (\xi_x^2 + \xi_y^2)^{1/2}$ are referred to as the degree of circular and (maximal) linear polarization, with $(P_{circ}^2 + P_{lin}^2)^{1/2}$ giving the total degree of polarization. Note that P_{circ} and P_{lin} are Lorentz-invariant quantities.

The Stokes parameter are related to polarization measurements in the following manner:

*) The term "vector" can be misleading since $\vec{\xi}$ does not transform as a vector.

$$\xi_x = -\left.\frac{\sigma_\parallel - \sigma_\perp}{\sigma_\parallel + \sigma_\perp}\right|_{(x,z)\text{-plane}}$$

$$\xi_y = -\left.\frac{\sigma_\parallel - \sigma_\perp}{\sigma_\parallel + \sigma_\perp}\right|_{(x=y,z)\text{-plane}} \tag{B2}$$

$$\xi_z = \frac{\sigma_L - \sigma_R}{\sigma_L + \sigma_R}$$

where $\sigma_\parallel$ and $\sigma_\perp$ are the cross sections for photons polarized in and out of the two respective (x,z)- and $(x = y, z)$-planes. Correspondingly $|\xi_x|$ and $|\xi_y|$ denote the degree of linear polarization in the two respective planes if $\xi_x < 0$ and $\xi_y < 0$, and out of the two respective planes if $\xi_x > 0$ and $\xi_y > 0$. σ_L and σ_R are the cross sections for left-handed (negative helicity) and right-handed (positive helicity) circular photons and $|\xi_z|$ denotes the degree of left-handed and right-handed circular polarization depending on whether $\xi_z > 0$ or $\xi_z < 0$, respectively.

For a partially polarized or elliptically polarized beam of photons there exist no single linear polarization plane. In these cases one defines a maximal linear polarization plane where the photon acquires its maximal degree of linear polarization $P_{lin} = (\xi_x^2 + \xi_y^2)^{1/2}$. The orientation of the maximal linear polarization plane can be obtained from the transformation law of the Stokes vector under a rotation $R_z(\varphi)$ around the z-axis

$$\begin{aligned}
\xi'_x &= \cos 2\varphi\, \xi_x + \sin 2\varphi\, \xi_y \\
\xi'_y &= -\sin 2\varphi\, \xi_x + \cos 2\varphi\, \xi_y \\
\xi'_z &= \xi_z
\end{aligned} \tag{B3}$$

which follows from the transformation behaviour of the density matrix under $R_z(\varphi)$ $\rho'_{\lambda\lambda'} = \rho_{\lambda\lambda'} \exp i(\lambda - \lambda')\varphi$. When $\xi'_y = 0$ the linear polarization will be entirely in the (x',z)-plane (or perpendicular to it) and have its maximal value $P_{lin} = (\xi_x^2 + \xi_y^2)^{1/2}$. The azimuth φ of the maximal linear polarization plane can be read off from (B3) and is given by $\mathrm{tg}\,\varphi = \xi_y/\xi_x$.

The density matrix of a pure polarization state

$$|e\rangle = a_+|+\rangle + a_-|-\rangle \quad (|a_+|^2+|a_-|^2=1) \tag{B4}$$

is given by

$$\rho_{\lambda\lambda'}^{(e)} = \begin{pmatrix} a_+a_+^* & a_+a_-^* \\ a_-a_+^* & a_-a_-^* \end{pmatrix} = \frac{1}{2}(\mathbb{1} + \hat{\xi}^{(e)}\cdot\vec{\sigma}) \tag{B5}$$

The probability W_e of measuring this pure state is then given by

$$W_e = \langle e|\rho|e\rangle = \mathrm{Tr}(\rho\rho^{(e)}) = \frac{1}{2}(1 + \vec{\xi}\cdot\hat{\xi}^{(e)}) \ . \tag{B6}$$

Consider a beam of photons where the azimuth of the maximal linear polarization plane is given by φ . Next consider a pure linear polarization analyser with azimuth ψ . The Stokes vector corresponding to this pure analyser is given by $\hat{\xi}^{(e)}=(\cos 2\psi, \sin 2\psi, 0)$. According to (B6) the probability distribution of this polarization analysis is given by

$$\frac{dW_e}{d\psi} = \frac{1}{2}(1 + P_{lin}\cos(2\varphi - 2\psi)) \tag{B7}$$

For a pure linearly polarized photon $P_{lin} = 1$ one recovers the classic angular distribution of a polarizer-analyser configuration $dW/d\psi = \cos^2(\varphi-\psi)$. The form of Eq.(B8) is also frequently used in the literature to represent the results of a polarization prediction. For an analyser with less than 100% analysing power $A_{lin} = (\xi_x^{A2} + \xi_y^{A2})^{1/2} < 1$ the distribution (B8) changes to $1/2(1+ A_{lin}\cdot P_{lin}\cos(2\varphi-2\psi))$.

In classical applications the Stokes vector is usually given in the Cartesian basis[27]. Consider a general unitary transformation on the helicity basis e_i ($e_1=e_+$, $e_2=e_-$) $e_i' = a_{ij}\, e_j$. The density matrix transforms according to

$$\rho'_{rs} = a^*_{mr}\rho_{mn}a_{ns} \tag{B8}$$

For the Stokes vector this implies

$$(\vec{\xi}'\cdot\vec{\sigma})_{rs} = a^*_{mr}(\vec{\xi}\cdot\vec{\sigma})_{mn}a_{ns} \tag{B9}$$

Specifically one has $e_x = (e_+ - e_-)/\sqrt{2}$ and $e_y = i(e_+ + e_-)/\sqrt{2}$ for the transformation from the helicity basis to the Cartesian basis. From (B9) the Stokes vector in the Cartesian basis is then given by

$$\begin{aligned} \eta_x &= -\xi_y \\ \eta_y &= \xi_z \\ \eta_z &= -\xi_x \end{aligned} \tag{B10}$$

where $\vec{\eta}$ and $\vec{\xi}$ are the Stokes vector in the Cartesian and helicity basis.

The Cartesian representation is more convenient for an interpretation of the physical content of polarization measurements. Consider again the probability W_e of (B6), but now in the Cartesian basis. Defining pairwise orthogonal pure polarization states e and $e_\perp$ with $e\cdot e_\perp = 0$ one has $\hat{\eta}^{(e)} = -\hat{\eta}^{(e_\perp)}$ and, according to (B6)

$$\vec{\eta}\cdot\hat{\eta}^{(e)} = W_e - W_{e_\perp} = \frac{d\sigma_e - d\sigma_{e_\perp}}{d\sigma_e + d\sigma_{e_\perp}} \tag{B11}$$

We shall list the Cartesian representation of the Stokes vector $\vec{\eta}$ of pure polarization states for some cases of interest: (i) $\hat{\eta} = (0,0,+(-)1)$ for linear polarization in the (x,z)- and (y,z)-planes (ii) $\hat{\eta} = (+(-)1,0,0)$ for linear polarization in the (x=y,z)- and (x=-y,z)-planes (iii) $\hat{\eta} = (0,+(-)1,0)$ for right- and left-handed circular polarization, i.e. positive and negative helicities, respectively. Using (B10) to transform to the helicity basis Stokes vector $\vec{\xi}$ one recovers the fundamental relation (B2) relating the components of $\vec{\xi}$ to polarization measurements.

Appendix C General Helicity Projection for $e^+e^- \to q\bar{q}g$

In the main text we have listed only the Born term helicity amplitudes for $e^+e^- \to q\bar{q}g$. For more general applications it is useful to avail of the general transformation between a set of invariant amplitudes and the helicity amplitudes. It is the purpose of this Appendix to present the relevant transformation matrix for helicity system IIa, where $p_{\bar{q}}$ is along the z-axis, and p_q lies in the(pos. x;z) half-plane.

The vector current matrix element for the production of a quark, antiquark and gluon with momenta p_1, p_2 and p_3 is defined as

$$\langle q(p_1)\bar{q}(p_2)g(p_3)|J^V_\mu(0)|0\rangle = \bar{u}(p_1)\Gamma_{\mu\nu}v(p_2)\varepsilon^*_\nu(p_3) \qquad (C1)$$

The axial vector current matrix element is defined accordingly with an extra γ_5 in (C1). In the following we shall deal only with the vector current case. The extension to the axial vector case is straightforward as described above.

The general covariant expansion of $\Gamma_{\mu\nu}$ is given by

$$\begin{aligned}\Gamma_{\mu\nu} = {} & B_1 g_{\mu\nu}\not{q} + B_2 p_{1\mu}\gamma_\nu + B_3 p_{2\mu}\gamma_\nu + B_4\gamma_\mu p_{2\nu} + B_5\gamma_\mu\gamma_\nu\not{q} \\ & + B_6 q_\mu\gamma_\nu + B_7\gamma_\mu q_\nu + C_1 p_{1\mu}p_{2\nu}\not{q} + C_2 p_{2\mu}p_{2\nu}\not{q} \qquad (C2) \\ & + C_3 q_\mu q_\nu\not{q} + C_4 q_\mu p_{2\nu}\not{q} + C_5 p_{1\mu}q_\nu\not{q} + C_6 p_{2\mu}q_\nu\not{q}\end{aligned}$$

Only covariants with an odd number of γ-matrices appear in the expansion because of γ_5-invariance for massless quarks.

Since from counting arguments there can be only 12 independent covariants in (C2), one has a linear relationship between the 13 covariants. This can be derived by noting that there are only 4 independent 4-vectors in 4-dimensional space-time [28]. One finds accordingly

$$\begin{aligned}& q^2\left[(1-x_3)g_{\mu\nu}\not{q} - x_2 p_{1\mu}\gamma_\nu + x_1 p_{2\mu}\gamma_\nu - (x_1+x_2)\gamma_\mu p_{2\nu} - (1-x_3)\gamma_\mu\gamma_\nu\not{q}\right] \\ & + 2p_{1\mu}p_{2\nu}\not{q} + 2p_{2\mu}p_{2\nu}\not{q} \\ & = q^2\left[(1-x_3)q_\mu\gamma_\nu - x_2\gamma_\mu q_\nu\right] + 2p_{2\mu}q_\nu\not{q} \qquad (C.3)\end{aligned}$$

Due to gauge invariance the invariant amplitudes in (C2) are subject to a number of gauge constraints resulting from $q_\mu\Gamma_{\mu\nu} = p_{3\nu}\Gamma_{\mu\nu} = 0$. These are given by

$$\begin{aligned}& B_1 + 2B_5 + B_7 + \tfrac{1}{2}q^2(2C_3 + x_1C_5 + x_2C_6) = 0 \\ & B_4 + \tfrac{1}{2}q^2(x_1C_1 + x_2C_2 + 2C_4) = 0 \\ & x_1B_2 + x_2B_3 - 2B_5 + 2B_6 = 0 \qquad (C4) \\ & B_1 + B_6 + \tfrac{1}{2}q^2(x_3C_3 + (1-x_1)C_4) = 0 \\ & -B_1 + B_2 - 2B_5 + \tfrac{1}{2}q^2((1-x_1)C_1 + x_3C_5) = 0 \\ & -B_1 + B_3 + \tfrac{1}{2}q^2((1-x_1)C_2 + x_3C_6) = 0 \\ & (1-x_1)B_4 + 2(1-x_2)B_5 + x_3B_7 = 0\end{aligned}$$

Judging from the 7 gauge constraints one will remain with 6 independent invariants describing $e^+e^- \to q\bar{q}g$, which of course agrees with the number of independent helicity amplitudes. As long as one is working in a perturbative context there is no point in constructing an explicit set of 6 gauge invariant

covariants since the complete set of Feynman diagrams in a given order is always gauge invariant. In practice one will always check gauge invariance explicitly through Eqs. (C4) and then proceed to work with the invariant amplitudes as defined by the expansion (C2). There is, however, one observation worth making in this context. Due to its simple structure the Born-term contribution (3.1) can only populate the lower dimensional covariants in (C.2) and thus $C_i = 0$ for the Born term, as is immediately obvious from Eq. (3.1). If one seeks a solution to the constraint equations (C4) only in terms of the invariants B_i, one finds one unique solution which, by necessity, has the Born term structure. Technically this comes about since the homogeneous constraint equation $M_{ij}B_j = 0$ derived from (C4) admits only 1 solution since the 7x7 constraint matrix M_{ij} can be checked to have rank 6 [8]. Thus, the gauge constraints are so restrictive that the Born term structure is already uniquely determined from these.

For the general helicity transformation we find

$$F^{\vee}_{\frac{1}{2}-\frac{1}{2}1;1} = (1-x_2)(1-x_3)\frac{\sqrt{(1-x_1)(1-x_2)}}{x_2x_3}\left[B_1 - B_2 + 2B_5 - \tfrac{q^2}{2}(1-x_1)C_1\right]$$

$$F^{\vee}_{\frac{1}{2}-\frac{1}{2}-1;1} = (1-x_1)\frac{\sqrt{(1-x_1)(1-x_2)}}{x_2x_3}\left[B_1 - (1-x_3)B_2 + 2B_5 + \tfrac{q^2}{2}(1-x_2)(1-x_3)C_1\right]$$

$$F^{\vee}_{-\frac{1}{2}\frac{1}{2}1;1} = (1-x_3)\frac{\sqrt{(1-x_1)(1-x_2)}}{x_2x_3}\left[(1-x_2)B_1 + (1-x_1)B_2 - x_2B_4 + 2B_5 - \tfrac{q^2}{2}(1-x_1)(1-x_2)C_1\right] \qquad (C5)$$

$$F^{\vee}_{-\frac{1}{2}\frac{1}{2}-1;1} = \frac{\sqrt{(1-x_1)(1-x_2)}}{x_2x_3}\left[(1-x_1)B_1 + (1-x_2)(1-x_3)B_2 + x_2(1-x_3)B_4 - 2(1-x_3)B_5 + \tfrac{q^2}{2}XC_1\right]$$

$$F^{\vee}_{\frac{1}{2}-\frac{1}{2}1;0} = \frac{1}{\sqrt{2}}(1-x_2)\frac{\sqrt{1-x_3}}{x_2x_3}\left[-2(1-x_1)B_1 + YB_2 + x_2^2B_3 + x_2(1-x_1)B_4 + 2(x_2-2(1-x_1))B_5 + \tfrac{q^2}{2}(1-x_1)YC_1 + \tfrac{q^2}{2}x_2^2(1-x_1)C_2\right]$$

$$F^{\vee}_{\frac{1}{2}-\frac{1}{2}-1;0} = \frac{1}{\sqrt{2}}(1-x_1)\frac{\sqrt{1-x_3}}{x_2x_3}\left[2(1-x_2)B_1 + YB_2 + x_2^2B_3 - x_2(1-x_2)B_4 + 2(2-x_2)B_5 - \tfrac{q^2}{2}(1-x_2)YC_1 - \tfrac{q^2}{2}x_2^2(1-x_2)C_2\right]$$

Here we have used the abbreviations $X = (1-x_1)(1-x_2)(1-x_3)$ and $Y = (1-x_1)(1-x_2) - (1-x_3)$. Note that in the c.m. helicity system IIa used here, only the 7 invariants $B_1,\ldots B_5$ and C_1, C_2 contribute to the helicity amplitudes. A convenient check on the helicity coefficients in each of the 6 equations (C5) is afforded by using the identity (C3).

Appendix D Transversity Frame Helicity Amplitudes

We write down transversity frame helicity amplitudes for a transversity frame where $p_{\bar{q}}$ is along x and p_q lies in the pos. (x,y) half plane. One has for the vector current helicity amplitudes

$$\begin{aligned}
F^{\vee}_{\frac{1}{2}-\frac{1}{2}1;1} &= x_1 e^{i\Theta_{12}/2}\\
F^{\vee}_{\frac{1}{2}-\frac{1}{2}-1;1} &= -x_2 e^{-i\Theta_{12}/2}\\
F^{\vee}_{-\frac{1}{2}\frac{1}{2}1;1} &= -x_2 e^{i\Theta_{12}/2}\\
F^{\vee}_{-\frac{1}{2}\frac{1}{2}-1;1} &= x_1 e^{3i\Theta_{12}/2}
\end{aligned} \qquad \otimes\, g_s\frac{\lambda^i}{2}\,\frac{1}{\sqrt{(1-x_1)(1-x_2)}}\,e^{i\Theta_{23}} \qquad (D1)$$

$$\begin{aligned}
F^{\vee}_{\frac{1}{2}-\frac{1}{2}1;0} &= \sqrt{2}\,x_1 e^{-i\Theta_{12}/2}\\
F^{\vee}_{\frac{1}{2}-\frac{1}{2}-1;0} &= \sqrt{2}\,x_2 e^{-i\Theta_{12}/2}
\end{aligned}$$

Except for the phase factors the transversity frame helicity amplitudes are rather simple. Note that the infrared-collinear singularities are now equally distributed amongst the six helicity amplitudes as one would expect, since the quantization axis z is perpendicular to the event plane.

The axial vector current helicity amplitudes are given by

$$F^{A}_{\lambda_q \lambda_{\bar{q}} \lambda_g ; \lambda} = -2\lambda_{\bar{q}} F^{V}_{\lambda_q \lambda_{\bar{q}} \lambda_g ; \lambda} \tag{D2}$$

and one has the Born term parity relations

$$F^{V}_{-\lambda_q -\lambda_{\bar{q}} -\lambda_g ; -1_0} = \pm F^{V\,*}_{\lambda_q \lambda_{\bar{q}} \lambda_g ; +1_0} \tag{D3}$$

The parity relations for the axial vector current helicity amplitudes F^A are the same as (D3) but with opposite signs.
Note that the parity relations are more involved if the underlying process is complex. We have checked by explicit calculation that the transversity frame cross-sections $\bar{\sigma}_\alpha$ calculated from (D1) and the helicity frame cross-sections $\bar{\sigma}_\alpha$(IIa) in Table 2 satisfy the general relations (2.17).

Appendix E Scalar Gluon Helicity Amplitudes

Since part of the predictions of QCD result from spin kinematics alone, it has become common practice to contrast the QCD predictions with the results of a scalar gluon theory. Although the scalar theory is not asymptotically

free, one can at least consistently handle the ultraviolet and infrared divergencies. In this Appendix we list all the relevant helicity amplitudes of interest involving scalar gluons. Cross-sections can be easily calculated by using the definitions of the main text.

1. $e^+e^- \to q\bar{q}S$

From the Feynman diagrams Fig. 2 one reads of

$$T^{V} = \bar{g}_s \frac{\lambda^i}{2} \bar{u}(p_1)\left[-\frac{(\not{p}_1+\not{p}_3)}{(p_1+p_3)^2}\gamma_\mu + \gamma_\mu \frac{(\not{p}_2+\not{p}_3)}{(p_2+p_3)^2}\right] v(p_2)$$
$$T^{A} = \bar{g}_s \frac{\lambda^i}{2} \bar{u}(p_1)\left[-\frac{(\not{p}_1+\not{p}_3)}{(p_1+p_3)^2}\gamma_\mu - \gamma_\mu \frac{(\not{p}_2+\not{p}_3)}{(p_2+p_3)^2}\right] \gamma_5 v(p_2) \tag{E1}$$

where $\bar{g}_s$ is the strong coupling constant of the scalar gluon theory (compare to (3.1)).

Note that T^V and T^A are not simply related. The helicity is flipped going from quark to antiquark,* i.e. $\lambda_q = \lambda_{\bar{q}}$. From helicity counting there are then only 6 vector and 6 axial-vector helicity amplitudes. Parity conservation implies

$$F^{V}_{-\lambda_q -\lambda_{\bar{q}} ; -1_0} = \pm F^{V}_{\lambda_q \lambda_{\bar{q}} ; +1_0} \tag{E2}$$

with the opposite signs for the corresponding relations between the axial-

* Even an infrared soft scalar gluon flips the helicity of the quark from which it is emitted. This means that the cancellation of infrared real and virtual infinities involves cross-sections with different helicity configurations in contradistinction to the vector gluon case. One concludes from this example that polarization measurements on quarks are not infrared safe in a scalar gluon theory.

vector helicity amplitudes F^A.

The quark-antiquark exchange relations corresponding to (3.6) read

$$F^{V,II a(b)}_{\alpha\beta;\sigma}(x_1,x_2,x_3) = F^{V,I b(a)}_{\beta\alpha;\sigma}(x_2,x_1,x_3)$$
$$F^{V,III a}_{\alpha\beta;\sigma}(x_1,x_2,x_3) = F^{V,III b}_{\beta\alpha;\sigma}(x_2,x_1,x_3) \qquad \text{(E3)}$$

where again the opposite signs hold for the corresponding relations between the axial vector helicity amplitudes F^A.

The resulting helicity amplitudes are listed in Table 6. We do not explicitly state the result of calculating the various cross sections σ_α and the longitudinal quark polarizations $\rho_{\alpha z}$ *. They can be easily written down from Table 6 if needed. Parity invariance and the reality of the Born term contribution limits the contributions to those listed in (3.5). However, in contrast to the vector gluon case, all four components of $H^i_{\mu\nu}$ (i = 1,..4) do contribute in general. Neither does one have a simple factorizing structure as in (3.7).

2. $e^+e^- \to Q\bar{Q}(1^{--}) \to SSS(\gamma SS)$

The matrix element for a polarized $Q\bar{Q}(1^{--}) \to SSS$ can be easily worked out from the Feynman diagram Fig. 3. For the helicity amplitudes $F_{\lambda_{QQ}}$ one

* Cross-sections for the purely electromagnetic case have been given in [29,30] which agree with the corresponding cross-sections calculated from Table 6.

obtains [18,31]

$$F_+ = 4\sqrt{2}\, N_{ijk} \frac{\sqrt{X}}{x_1^2 x_2 x_3}(3x_1-2)$$
$$F_0 = 8 N_{ijk} \frac{1}{x_1^2 x_2 x_3}(x_2-x_3)(2x_1-1) \qquad \text{(E4)}$$

where $N_{ijk} = \frac{1}{2} f_{ijk} (\bar{\alpha}_s 4\pi)^{3/2} N$, and N is the normalization factor (4.2) and where $\bar{\alpha}_s$ is the coupling constant of the scalar gluon theory. The parity condition reads $F_- = -F_+$. Bose symmetry requires $F_+ (F_0)$ to be symmetric (antisymmetric) under $x_2 \leftrightarrow x_3$. The helicity amplitudes $F_{\lambda\gamma;\lambda_{Q\bar{Q}}}$ for $Q\bar{Q}(1^{--}) \to \gamma SS$ are given by

$$F_{+;+} = -8 N_{ij} \frac{1}{x_1^2 x_2 x_3}\left(x_1(1-x_2x_3) - X\right)$$
$$F_{-;+} = -8 N_{ij} \frac{1}{x_1^2 x_2 x_3} X \qquad \text{(E5)}$$
$$F_{+;0} = 4\sqrt{2}\, N_{ij} \frac{1}{x_1^2 x_2 x_3} \sqrt{X}(x_2-x_3)$$

where $N_{ij} = \delta_{ij} \sqrt{\alpha^{-1}} \bar{\alpha}_s (4\pi)^{3/2} Q_f^2 N$. The parity conditions are $F_{-\lambda\gamma;-} = F_{\lambda\gamma;+}$ and $F_{-\lambda\gamma;0} = -F_{\lambda\gamma;0}$. Bose symmetry determines $F_{\lambda\gamma;+}$ $(F_{\lambda\gamma;0})$ to be symmetric (antisymmetric) under $x_2 \leftrightarrow x_3$. The correlation cross-sections σ_α and the linear polarization components of the photon resulting from (E5) have been discussed in [18].

References

1. JADE Collaboration, W. Bartel et al., Phys. Lett. 91B (1980) 142.
   MARK-J Collaboration, D.P. Barber et al., Phys. Rev. Lett. 43 (1979) 830.
   PLUTO-Collaboration, Ch. Berger et al., Phys. Lett. 86B (1979) 418.
   TASSO Collaboration, R. Brandelik et al., Phys. Lett. 86B (1979) 243.

2. Ch. Berger et al., Phys. Lett. 82B (1979) 449.

3. G. Kramer, G. Schierholz and J. Willrodt, Phys. Lett. 78B (1978) 249;
   Erratum ibid. 80B (1979) 433.

4. K.Koller,H.Krasemann and T.F.Walsh,Z.Phys.C1(1979)71.
   K.Koller and T.F.Walsh,Nucl.Phys.B140(1978)449.

5. G.Schierholz and D.H.Schiller,Preprint DESY 80/88(1980).For related work see H.A.Olsen,P.Osland and I.Øverbø,Nucl.Phys.B171(1980)209.

6. C.Bourrely,E.Leader and J.Soffer,Phys.Reports,59(1980)95.

7. A.De Rújula,R.Petronzio and B.Lautrup,Nucl.Phys.B146(1978)50.

8. J.G.Körner,G.Kramer,G.Schierholz,K.Fabricius and I.Schmitt,Phys.Lett. 94B(1980)207; K.Fabricius and I.Schmitt,Z.Phys.C3(1979)51.

9. G.Schierholz and D.H.Schiller,Preprint DESY 79/29(1979),unpublished.

10. J.Ellis,M.K.Gaillard and G.Ross,Nucl.Phys.B111(1976)253.

11. K.Koller,D.H.Schiller and D.Wähner,Preprint DESY 80/99(1980).

12. J.F.Nieves,Phys.Rev.D20(1979)2775;
    J.E.Augustin and F.M.Renard,Nucl.Phys.B162(1980)341;
    A.Bartl,H.Fraas and W.Majerotto,Z.Physik C6(1980)335.

13. O.Nachtmann, Nucl.Phys.B127(1977)314.

14. H.A.Olsen,P.Osland and I.Øverbø,Phys.Lett.89B(1980)221.

15. T.A.deGrand and B.Petersson,Phys.Rev.D21(1980)3129

16. S.J.Brodsky,T.A.deGrand and R.F.Schwitters,Phys.Lett.79B(1978)255.

17. R.Delbourgo,A.Salam and J.Strathdee,Proc.Roy.Soc.A278(1965)146;
    B.Sakita and K.Wali,Phys.Rev.Lett.14(1965)404.For a quark model formulation see T.Gudehus,DESY Report 68/11 (1968),unpublished and Phys.Rev.184,1788 (1969).

18. J.G.Körner and D.McKay, Z.Phys.C9, 67(1981).

19. M.Krammer,Phys.Lett.74B(1978)361

20. G.Alexander et al.,Phys.Lett.76B(1978)652.

21. K.Fabricius, I.Schmitt,G.Kramer and G.Schierholz,Phys.Rev.Lett.45(1980)867.

22. L.M.Sehgal and P.M.Zerwas,Aachen Preprint PITHA 11(1980).

23. K.Koller,K.H.Streng,T.F.Walsh and P.M.Zerwas,Preprint DESY 80/132(1980).

24. A.Ali,J.G.Körner,Z.Kunszt,E.Pietarinen,G.Kramer,G.Schierholz and J.Willrodt,Phys.Lett.82B(1979)285 and Nucl.Phys.B167(1980)454;
    J.G.Körner,G.Schierholz and J.Willrodt,Preprint DESY 80/119(1980);
    T.Chandramohan and L.Clavelli,Phys.Lett.94B(1980)409 and Preprint BONN-He-80-22; K.J.F.Gaemers and J.A.M.Vermaseren,Z.Physik C7(1980)81.

25. M.Jacob and G.Wick,Ann.Phys.7(1959)404.

26. P.R.Auvil and J.J.Brehm,Phys.Rev.145(1966)1152.

27. M.Born and E.Wolf,Priciples of Optics(Pergamon Press,Oxford,1975);
    L.D.Landau and E.M.Lifschitz,Klassische Feldtheorie,§ 50 (Akademie-Verlag Berlin,1973);
    H.A.Olsen,in Springer Tracts in Modern Physics,vol.44,p.83 (Springer-Verlag Berlin,1968).

28. M.Perrottet,Nuovo Cimento Lett.7(1973)915.

29. G.Schierholz,Proc.SLAC Summer Institute on Particle Physics, Quantum Chromodynamics,1979, ed.A.Mosher,p.476.

30. K.Koller,H.G.Sander,T.F.Walsh and P.M.Zerwas,Z.Physik C6(1980)131.

31. K.Koller and H.Krasemann,Phys.Lett.88B(1979)119.

32. H.A.Olsen,P.Osland and I.Øverbø,Preprint NORDITA-81/13(April 1981).

Figure Captions

Fig.1 Relative orientation of the beam frame Ox'y'z' (with z' along the electron beam and x' in the accelerator plane pointing inward) and the helicity rest frames $Ox_{\pm}y_{\pm}z_{\pm}$ of $e^{\pm}$.

Fig.2 Definition of the Euler angles φ, θ and χ relating the beam frame Ox'y'z' and the event frame Oxyz. The three successive Euler rotations are $R_{\hat{z}'}(\varphi)$ followed by $R_{\hat{y}_1}(\theta)$ and then by $R_{\hat{z}}(\chi)$.

Fig.3 Feynman diagrams for $e^+e^- \to q(p_1)\bar{q}(p_2)g(p_3)$.

Fig.4 Born term diagram for $Q\bar{Q}(1^{--}) \to ggg$.

$F^V_{\lambda_q\lambda_{\bar{q}}\lambda_g;\sigma}$	Ia	IIa	IIIa
Transverse F_T^V			
1/2 -1/2 1; 1	$(1-x_3)$	0	$-(1-x_1)$
1/2 -1/2 -1; 1	$-x_1^2$	$-(1-x_1)(1-x_2)$	$(1-x_1)(1-x_3)$
-1/2 1/2 1; 1	0	$-(1-x_3)$	$(1-x_2)$
-1/2 1/2 -1; 1	$(1-x_1)(1-x_2)$	x_2^2	$-(1-x_2)(1-x_3)$
Longitudinal F_L^V			
1/2 -1/2 1; 0	$-\sqrt{2X}$	0	$-\sqrt{2X}$
1/2 -1/2 -1; 0	0	$\sqrt{2X}$	$\sqrt{2X}$

Table I: Vector current helicity amplitudes for $e^+e^- \to q\bar{q}g$. Entries to be multiplied by $2g_s \frac{\lambda^i}{2}/(x_j(1-x_1)^{1/2}(1-x_2)^{1/2})$ where $x_j = x_1, x_2, x_3$ in system I, II and III, respectively. $X = (1-x_1)(1-x_2)(1-x_3)$. Amplitudes for systems Ib, IIb and IIIb given by the replacement $F_T \to F_T$ and $F_L \to -F_L$. Axial-vector current helicity amplitudes related to entries by (3.4).

σ_α	Ia	IIa	IIIa
σ_{U+L}^{VV}	$2\,\frac{x_1^2+x_2^2}{(1-x_1)(1-x_2)}$	$2\,\frac{x_1^2+x_2^2}{(1-x_1)(1-x_2)}$	$2\,\frac{x_1^2+x_2^2}{(1-x_1)(1-x_2)}$
σ_L^{VV}	$4\,\frac{1-x_3}{x_1^2}$	$4\,\frac{1-x_3}{x_2^2}$	$8\,\frac{1-x_3}{x_3^2}$
σ_T^{VV}	$\sigma_T^{VV} = \frac{1}{2}\sigma_L^{VV}$		
σ_I^{VV}	$\sqrt{2X}\,\frac{(1-x_1)(1-x_2)-(1-x_3)}{x_1^2(1-x_1)(1-x_2)}$	$-\sqrt{2X}\,\frac{(1-x_1)(1-x_2)-(1-x_3)}{x_2^2(1-x_1)(1-x_2)}$	$-\sqrt{2X}\,\frac{x_1^2-x_2^2}{x_3^2(1-x_1)(1-x_2)}$
σ_7^{VA}	$2\,\frac{x_1(x_1^2-x_2^2)+2(1-x_3)x_2}{x_1(1-x_1)(1-x_2)}$	$-2\,\frac{(x_2(x_2^2-x_1^2)+2(1-x_3)x_1}{x_2(1-x_1)(1-x_2)}$	$-2\,\frac{(x_1-x_2)(1+(1-x_3)^2)}{x_3(1-x_1)(1-x_2)}$
σ_8^{VA}	$-\sqrt{2X}\,\frac{x_1x_2}{x_1^2(1-x_1)(1-x_2)}$	$-\sqrt{2X}\,\frac{x_1x_2}{x_2^2(1-x_1)(1-x_2)}$	$\sqrt{2X}\,\frac{x_3(x_1+x_2)}{x_3^2(1-x_1)(1-x_2)}$

Table 2: $e^+e^- \to q\bar{q}g$ correlation cross sections σ_α in coordinate systems Ia, IIa IIIa. Entries to be multiplied by 16 g_s^2. For systems Ib, IIb and IIIb σ_I^{VV} and σ_8^{VA} change sign and the other σ_α remain unchanged.
$X = (1-x_1)(1-x_2)(1-x_3)$.

α		$\sigma_\alpha(\mathrm{IIIa})$	$S_{\alpha x}(\mathrm{IIIa})$	$S_{\alpha y}(\mathrm{IIIa})$	$S_{\alpha z}(\mathrm{IIIa})$
U	VV	s	$-4(1-x_3)\left[(1-x_1)^2+(1-x_2)^2\right]$	-	-
	VA	-	-	0	$-2x_3^2(x_1^2-x_2^2)$
L	VV	s	$-8X$	-	-
	VA	-	-	0	zero
T	VV	s	$-2(1-x_1)(1-x_2)(1+(1-x_3)^2)$	-	-
	VA	-	-	0	zero
4	VV	-	-	$-2(1-x_1)(1-x_2)x_3(x_1+x_2)$	0
	VA	0	0	-	-
5	VV	-	-	$\sqrt{2X}\,(x_1-x_2)x_3$	0
	VA	0	0	-	-
I	VV	a	$\sqrt{2X}(x_1^2-x_2^2)$	-	-
	VA	-	-	0	$\sqrt{2X}\,x_3^2$
7	VV	-	-	$-2x_3(x_1+x_2)\left[(1-x_1)^2+(1-x_2)^2\right]$	
	VA	a	$4x_3(1-x_3)(x_1-x_2)$	-	-
8	VV	-	-	0	$-\sqrt{2X}\,x_3(x_1-x_2)$
	VA	s	$-\sqrt{2X}\,x_3(x_1+x_2)$	-	-
9	VV	0	0	-	-
	VA	-	-	$-\sqrt{2X}\,x_3^2$	0

Table 3: $e^+e^- \to q\bar{q}g$ correlation Stokes vectors of the gluon in system IIIa. $X = (1-x_1)(1-x_2)(1-x_3)$. All entries - except σ_α given in Table 2 - to be multiplied by $16\,g_s^2/(x_3^2(1-x_1)(1-x_2))$. In σ_α-column s(a) indicates symmetric (antisymmetric) under $x_1 \leftrightarrow x_2$. Zero contributions are denoted by: (-) if due to parity; (0) if due to reality of the Born terms (T-odd elements) and (zero) if due to charge conjugation (3.6). For system IIIb change sign of the entries with index α = 5,I,8 and 9.

$F_{\lambda_1\lambda_2\lambda_3;\lambda_{Q\bar{Q}}}$					
F_T:	+++;+	0	F_L:	+++;0	0
	++−;+	$(1-x_2)(1-x_3)$		++−;0	$\sqrt{2X}\,(1-x_3)$
	+−+;+	$(1-x_2)(1-x_3)$		+−+;0	$-\sqrt{2X}\,(1-x_2)$
	+−−;+	$(1-x_1)x_1^2$		+−−;0	0
	−++;+	0			
	−+−;+	$(1-x_1)(1-x_2)^2$			
	−−+;+	$(1-x_1)(1-x_3)^2$			
	−−−;+	0			

Table 4: Helicity amplitudes for quarkonium decay into 3g or γgg. Entries to be multiplied by $\frac{1}{4}N_{ijk}/(x_1^2x_2x_3)$, with N_{ijk} given in (4.2) for 3g-decay and replaced by N_{ij} from (4.2') for γgg-decay. $X = (1-x_1)(1-x_2)(1-x_3)$.

α	σ_α	$\rho_{\alpha x}$	$\rho_{\alpha y}$	$\rho_{\alpha z}$
U+L	$2x_1^2\sum_{i=1}^{3}x_i^2(1-x_i)^2$	$4x_1^2X$	−	−
L	$4X\left[(1-x_2)^2+(1-x_3)^2\right]$	$8\,X(1-x_2)(1-x_3)$	−	−
T	$\sigma_T=\frac{1}{2}\sigma_L$	$2(1-x_2)^2(1-x_3)^2(1+(1-x_1)^2)$	−	−
4	−	−	$2(1-x_2)^2(1-x_3)^2x_1(x_2+x_3)$	0
5	−	−	$-\sqrt{2X}\,(1-x_2)(1-x_3)x_1(x_2-x_3)$	0
I	$\sqrt{2X}\left[(1-x_2)(1-x_3)(x_2-x_3)+(1-x_1)((1-x_2)^3-(1-x_3)^3)\right]$	$-\sqrt{2X}\,(1-x_2)(1-x_3)(x_2^2-x_3^2)$	−	−
7	−	−	0	$4x_1(1-x_2)(1-x_3)\left[2x_1(1-x_1)^2+(1-x_2)(1-x_3)(x_2+x_3)\right]$
8	−	−	0	$-\sqrt{2X}\,x_1\left[x_2(1-x_2)^2-x_3(1-x_3)^2\right]$
9	0	0	−	−

Table 5: Correlation density matrix elements of gluon 1 (most energetic) or photon in quarkonium decay. Entries to be multiplied by $\frac{1}{4}N_{ijk}^2/(x_1^4x_2^2x_3^2)$ for 3g-decay and by $\frac{1}{4}N_{ij}^2/(x_1^4x_2^2x_3^2)$ for γgg-decay. $X = (1-x_1)(1-x_2)(1-x_3)$. Zero contributions denoted as in caption to Table 3.

$F_{\lambda_q\lambda_{\bar{q}};\sigma}$	Ia	IIa	IIIa
$F^V_{\frac{1}{2}\frac{1}{2};1}$	$(1-x_2)$	$(1-x_1)$	0
$F^V_{-\frac{1}{2}-\frac{1}{2};1}$	$(1-x_1)(1-x_3)$	$(1-x_2)(1-x_3)$	$-x_3^2$
$F^V_{\frac{1}{2}\frac{1}{2};0}$	$\sqrt{2X}$	$-\sqrt{2X}$	0
$F^A_{\frac{1}{2}\frac{1}{2};1}$	$(1-x_2)(2x_1-1)$	$-(1-x_1)(2x_2-1)$	0
$F^A_{-\frac{1}{2}-\frac{1}{2};1}$	$(1-x_1)(1-x_3)$	$-(1-x_2)(1-x_3)$	$x_3(x_1-x_2)$
$F^A_{\frac{1}{2}\frac{1}{2};0}$	$-\sqrt{2X}\,(1-x_1)$	$-\sqrt{2X}\,(1-x_2)$	$-\sqrt{2X}\;x_3$

Table 6: Vector and axial vector current helicity amplitudes for $e^+e^- \to q\bar{q}S$. Entries to be multiplied by $\sqrt{2}\,\bar{g}_{s\bar{2}}^{\lambda^i}/(x_j(1-x_1)^{1/2}(1-x_2)^{1/2})$, where $x_j = x_1, x_2, x_3$ in system I, II and III, respectively. $X = (1-x_1)(1-x_2)\cdot(1-x_3)$. Amplitudes for systems Ib, IIb and IIIb given by the replacement $F_T \to F_T$ and $F_L \to -F_L$.

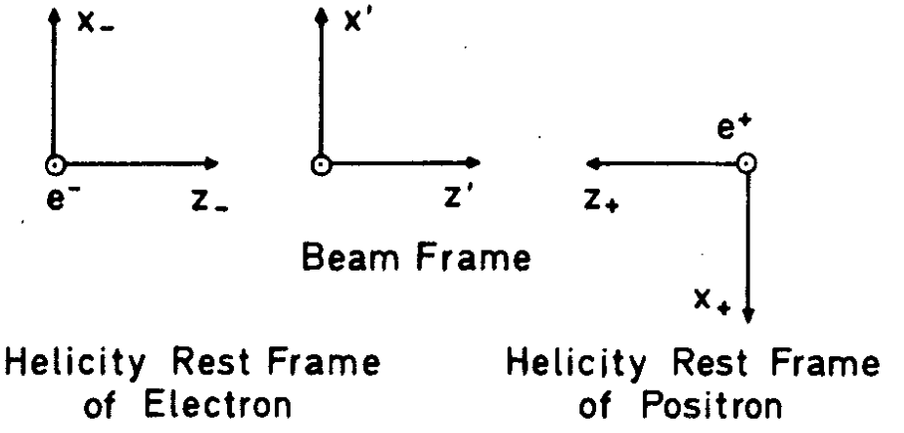

Fig.1

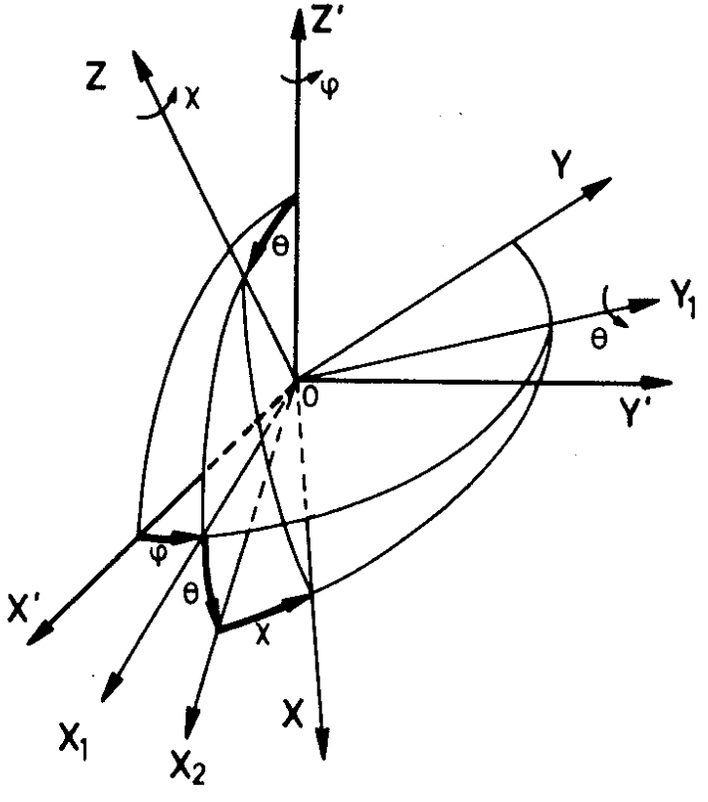

Fig. 2

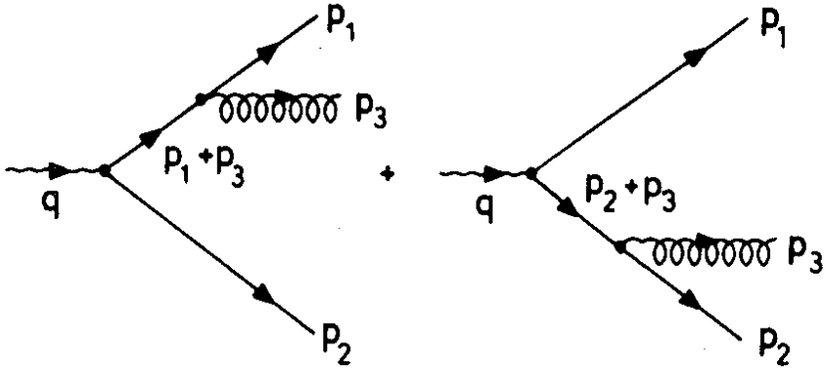

Fig.3

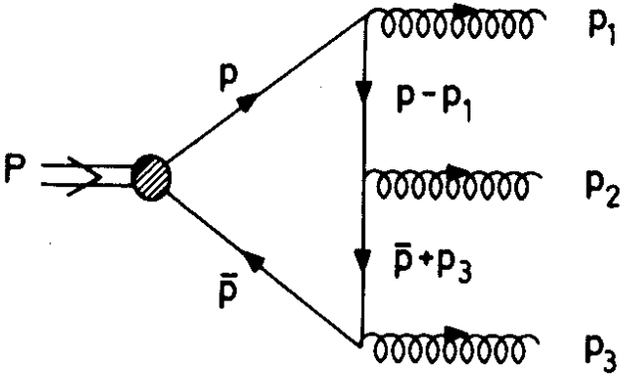

+ 5 permutations

Fig. 4